SYNTHESIS AND CHARACTERIZATION OF MgO/ZnO NANOCOMPOSITE MODIFIED CARBON PASTE ELECTRODE FOR THE DETERMINATION OF CADMIUM AND LEAD IN MILK

MSc THESIS

MESFIN TESHOME KEBEDE

FEBRUARY 2018

HARAMAYA UNIVERSITY, HARAMAYA

Synthesis and Characterization of MgO/ZnO Nanocomposite Modified Carbon Paste Electrode for Determination of Cadmium and Lead in Milk

MSc Thesis Submitted to the Department of Chemistry, Postgraduate Program Directorate

HARAMAYA UNIVERSITY

In partial Fulfillment of the Requirements for the Degree of

MASTER OF SCIENCE IN CHEMISTRY

Mesfin Teshome Kebede

FEBRUARY 2018

Haramaya University, Haramaya

HARAMAYA UNIVERSITY

POSTGRADUATE PROGRAM DIRECTORATE

As Thesis Research advisors,we hereby certify that we have read and evaluated this thesis prepared under our guidance, by **Mesfin Teshome Kebede**, entitled: **Synthesis and Characterization of MgO/ZnO Nanocomposite Modified Carbon Paste Electrode the Determination of Cadmium and Lead in Milk** and we recommend that it be submitted as fulfilling the Thesis requirement

Abebaw Adgo (PhD) _____ _____

Major Advisor Signature Date

Endale Teju (PhD) _____ _____

Co-advisor Signature Date

As a member of the board of examiners of the MSc Thesis Open Defense Examination, I certify that I have read and evaluated the Thesis prepared by Mesfin Teshome and examined the candidate. I recommend that the Thesis be accepted as fulfilling the Thesis requirement for the degree of **Master of Science in Chemistry**.

_____ _____ _____

Chairperson Signature Date

_____ _____ _____

Internal Examiner Signature Date

_____ _____ _____

External Examiner Signature Date

DEDICATION

I dedicate this thesis manuscript to my beloved family and my wife **Meseret Tesfaye** for their continuous support and encouragement during my study.

STATEMENT OF THE AUTHOR

By my signature below, I declare and affirm that this Thesis is my own work. I have followed all ethical and technical principles of scholarship in the preparation, data collection, data analysis and compilation of this Thesis. Any scholarly matter that is included in the Thesis has been given recognition through citation.

This Thesis is submitted in partial fulfillment of the requirements for an MSc degree at the Haramaya University Library and is made available to borrowers under the rules of the Library. I solemnly declare that this Thesis has not been submitted to any other institution anywhere for the award of any academic degree, diploma or certificate.

Brief quotations from this Thesis may be made without special permission provided that accurate and complete acknowledgment of the source is made. Requests for permission for extended quotation from or reproduction of this Thesis in whole or part may be granted by the Head of the Department or postgraduate program directorate when in this or her judgment the proposed use of material is in the interest of scholarship. In all other instances, however, permission must be obtained from the author of the Thesis.

Name: **Mesfin Teshome Kebede** **Signature_____**

Place: **Haramaya University**

Date: **November 2017**

Department: **Chemistry**

BIOGRAPHICAL SKETCH OF THE AUTHOR

The author was born in Oromia Regional State, Arsi Zone, and Marti Woreda from his father Teshome Kebede and his mother Mulu Nigusse, on June 12, 1986. He attended his elementary school at Moleme Saka and Gora Terara Elementary School and his secondary and preparatory School at Arbegnoch Senior Secondary School, Abomsa. After completing preparatory school, he joined Hawassa University, Department of Chemistry in 2005/06 and graduated with BSc degree in Chemistry in 2008. Soon after graduation, the author was employed by Ministry of Education in 2008 to work under Oromia Education Bureau, in Arsi zone, Chole Woreda, Chole preparatory school as a teacher. After five years service, he joined Haramaya University, College of Natural and Computational Sciences, Department of Chemistry in 2013 to pursue his postgra duate studies in Chemistry, under the Non-regular Postgraduate program.

ACKNOWLEDGEMENTS

In accomplishing this Thesis work, many efforts have been put together to bring it to its final. First and foremost, I would like to express my deepest heartfelt gratitude to my advisor Dr. Abebaw Adgo for his limitless help, continuous, excellent and timely advices, valuable and constructive comments, close follow or supervision throughout my work and reading the manuscript. This Thesis work would have not been completed without his valuable comments and suggestions.

Secondly, my special heartfelt thanks also goes to may Co-advisor Dr. Endale Teju for his close fatherly approach, guidance, coordination, valuable comments, suggestions, encouragement and in correcting my paper including the proposal and many other unlisted and uncountable supports which are unforgettable.

I would like to express my deepest appreciation and thanks to Haramaya University and Chemistry Department for giving me this opportunity to complet this post graduate study program. I gratefully acknowledge Ministry of Education for the financial support and Haramaya University Research Laboratory, Addis Ababa University Department of Chemistry for characterization of the nano particle using XRD and FTIR, and Leather Developmental Institute of Ethiopia for morphological of characterization the as-sensitized powder using Scanning Electron Microscope.

My special thanks also go to my wife Meseret Tesfaye, my father Ato Teshome Kebede and my Mother W/ro Mulu Nigussie and all my brothers and sisters for their continuous encouragement. Finally I wish to thank my friends for all their help, support and guidance.

At last, but not least, my acknowledgment and grateful appreciation goes to all Chemistry Department staff members for their friendly treatment specially Ato Fituma Diriba, Kassie Dessallegn,Yanchamlak Adamu and Woyineshet Alamaw for their voluntary assistance and cooperation during laboratory experimental works by scarifying their extra time and providing the desired laboratory equipments and cooperation in various steps of this work and all people who helped me in completing my Thesis work.

ABBREVIATIONS AND ACRONYMS

AAS	Atomic Absorption Spectroscopy
ASV	Anodic Stripping Voltammetric
CPEs	Carbon Paste Electrodes
CV	Cyclic Voltammetry
EPA	Environmental Protection Agency
ESA	Electrochemical Stripping Analysis
FAO	Food Agriculture Organization
GCE	Glassy Carbon Electrode
LSSV	Linear Sweep Stripping Voltammetry
MCPEs	Modified Carbon Paste Electrodes
NCPs	Nanocomposites
NPs	Nanoparticles
SEM	Scanning Electron Microscopy
SV	Stripping Voltammetry
SVS	Stripping Voltammetry System
WHO	World Health Organization
XRD	X-Ray Diffraction

TABLE OF CONTENTS

Continuous

Continuous

LIST OF TABLES

Tables **Pages**

LIST OF FIGURES

Figures **Pages**

LIST OF TABLES IN THE APPENDIX

LIST OF FIGURE IN THE APPENDIX

Synthesis and Characterization of MgO/ZnO Nanocomposite Modified Carbon Paste Electrode for the Determination of Cadmium and Lead in Milk

ABSTRACT

Magnesium oxide/zinc oxide nanocomposite was synthesized using hydrothermal methods from $Mg(NO_3)_2.6H_2O$ and $Zn(NO_3)_2.6H_2O$ precursor salts. The morphology, structure and composition of the nanocomposite were characterized by employing FTIR, SEM, XRD and Uv-vis spectroscopy. The SEM image showed a uniform distribution of nanosheet of ZnO and irregular shape of MgO nanoparticles. Also the XRD and the EDX result showed that the synthesis nanocomposite was purely MgO/ZnO. An electrochemical property of MgO/ZnO composite modified carbon paste electrode (CPE) was studied using cyclic voltammetry in the presence of 2 M potassium ferrocynide +0.1 M KCl. The MgO/ZnO modified CPE highly reversible than the bare CPE and single system modified CPE. The active surface area of carbon paste electrode was significantly improved with 1.7 fold by the nanocomposite. The modified CPE optimized condition was found to be pH 4.5, deposition potential was -0.6 and - 0.9V for Pb and Cd ions, respectively, deposition time 90s and 400 ppm concentration for both metals. Under the optimized conditions, MgO/ZnO modified CPE was utilized for the determination of Lead and Cadmium in milk samples using anodic stripping voltammetry. The sensor exhibited 100 – 800 ppm linear range; the sensitivity of Cd and Pb was 0.817 and 0.797 respectively and detection limit for both metal ions was 0.45µg/L for Cd and 0.142µg/L for Pb. Besides, compared with CPE, MgO/ZnO modified CPE exhibited well-defined and separate peaks for Cd and Pb. The modified CPE electrode was also applied for the determination of the two metals in milk; the obtained result was less than the maximum allowed limits. The modified CPE electrode displayed good sensitivity and selectivity for Pb and Cd detection. Therefore, MgO/ZnO nanocomposite modified CPE could be a potential candidate for the determination of trace heavy metals and holding great promise for routine analysis.

Keywords: Anodic stripping voltammetry, Toxic heavy metals, Magnesium oxide, Zinc oxide, Nanocomposite, Carbon paste electrode, Milk

1. INTRODUCTION

Cow milk is an important food of animal origin; it has most of the nutrients necessary for a healthy diet, and is an important food for some consumer groups, such as infants and the elderly. Heavy metals accumulate in the food chain, so all foodstuffs, especially products of animal origin, become unsafe as heavy metal pollution increases. It has been reported that the content of the main elements in milk are fairly constant and undergoes slight changes depending on lactation phase, quality of nutrition and environmental conditions mainly chemical pollutants (Dobrzanski *et al*., 2005). The amount of metals in cow milk is widely studied, particularly in industrialized and polluted areas of the developed and the developing countries of the world since animals grazed freely on open fields are considered as bio-indicators of environmental pollution (LI-Quang *et al*., 2009). Metal level in uncontaminated milk is generally low, but by inhalation of polluted air, intake of contaminated feeds and absorption through the skin, many dangerous elements or compound such as metals and metalloid, accumulate along the food chain (Binghila *et al*., 2008). Therefore, the determinate on of levels of toxic heavy metals in milk is great importance.

The level of toxic heavy metal has been determined using spectroscopic methods, such as atomic absorption spectrometry (AAS), X-ray fluorescence spectrometry and Graphite Furnace Atomic Absorption Spectrometry (Chuparina and Aisueva, 2011). Prticularly Cd and Pb were determined by Graphite Furnace Atomic Absorption Spectrometry with the detection limit of 1×10^{-4} µ/g and 0.001µ/g, respectively (Józef Szkoda and Jan Żmudzki, 2005). These methods however, require complex sample pretreatment processes and are expensive for routine applica tions, in addition to these other alternative method for analysis of trace heavy metal ions is electrochemical (Zhengcui *et al*., 2013). They developed these materials for sensitive and simple for the rapid evaluation of heavy metal levels which are highly desirable for environmental monitoring and food safety applications. Compared with an optical instrument, electrochemical devices are relatively cost effective and miniaturizable. Electrochemical methods, especially electrochemical stripping analysis (ESA) instruments are portable, compact and inexpensive compared to spectroscopic equipment, and are thus practical for on-site measurements for biomedical, environmental and industrial monitoring (Tesarovaa *et al.*, 2009). The other advantage of using voltammetric technique is that the sample is taken

automatically and analysis is performed immediately without the need to collect a sample manually risking contamination and metal loss (Brainina *et al.*, 2009) and has extremely low detection limits and also works in the presence of high salt concentration. ESA are widely recognized as a powerful tool for the simultaneous determination of multiple types of metal ion, because of the combination of an effective pre concentration step with advanced electrochemical measurements of the accumulated analytes (Economou, 2005). The stripping voltammetry system (SVS) in combination with modified carbon paste electrode is designed for suitable and continuous monitoring with sufficient sensitivity and avoids the use of toxic mercury (Mikkelson and Schroder, 2004).

Mercury electrodes have high reproducibility and sensitivity, are therefore, preferred for stripping analysis (Wu *et al*., 2008). However, the toxicity of mercury makes it undesirable for certain sensing applications, particularly those involving food contacts. Considerable efforts have been made to find suitable alternative electrode materials for stripping analysis. Recently, bismuth film electrodes (BiFEs) have been proposed in view of their low toxicity and comparable performance to mercury (Ping *et al*., 2011). However, BiFEs have a serious limitation because of insufficient adhesion of the film on the electrode surface which causes degradation of the electrode (Hwang *et al*., 2008).

Chemically modified carbon paste electrodes (MCPEs) are cheap, easy to make, and have a low background current, and so have been originally designed as an alternative to mercury electrode. Metallic or metal oxide nano particles have been successfully employed to modify CPEs for stripping analysis (Švancara *et al.*, 2009). However, the inherent disadvantages of CPEs such as low mechanical stability and reproducibility limit their practical application. Therefore, new electrode material developments are still needed to meet the growing demands for on-site monitoring of trace heavy metal ions. Nanostructure materials are candidates because of their large specific surface area, good biocompatibility, and ease of preparation. Nanomaterial modified CPEs exhibit many favorable characteristics for electro analysis, including fast response, high sensitivity, selectivity, low back ground current, low cost, suitable for use in the field, has wide (broad) potential window and long time stability, their low ohmic resistance and easy preparation (Lahiff *et al.*, 2010). The CPE can be modified using metal oxide nanoparticles. Nanostructured metal oxides such as ZnO, Fe_3O_4,

NiO, SnO_2, ZrO_4, TiO_2, Al_2O_3, MgO and MnO_2 have also been widely used in the detections of toxic heavy metals due to their interesting nanomorphological, functionally biocompatible and catalytic properties. These materials exhibit enhanced electron transfer kinetics and strong adsorption capability. For example, porous MgO nano flowers have been synthesized was to fabricate the heavy metal sensitive electrode (Wei *et al*., 2012). The detection of toxic heavy metal ion using stripping voltammetry by new nonmaterial with highly selective adsorption toward a specific metal ion should be a great interest and significance (Wei *et al*., 2012). MgO nonmaterial, as a non-toxic and environmentally friendly material, has been widely used as an absorbent to remove toxic metals ions and organic pollutants from water due to its high surface reactivity and adsorption capacity toward Pb(II) and Cd(II) (Yan *et al*., 2012).

By combining with squarewave anodic stripping voltammetry the modified electrode exhibits excellent sensing performance for Pb^{2+} and Cd^{2+} with detection limits of 2.1 pM and 8.1 pM, respectively (Lin *et al*., 2015). MgO/ZnO composite nanosheet could be used as good (Jianwei *et al*., 2015). Zinc oxide nanoparticles synthesized by hydrothermal method have been investigated for the removal of Cd(II) and other heavy metal ions from aqueous solution with good removal efficiency (Yantasee *et al*., 2008).

Therefore a novel carbon paste electrode modified with magnesium oxide/ zinc oxide nanocomposite (ZnO/MgONCPs) is excellent for detection of toxic heavy metal ions. Such a composite electrode brings new capabilities for electrochemical devices by combining the unique advantages of nanomaterials with the characteristics of a bulk composite electrode. It is better to modified CPE by MgO/ZnONCPs for detection of toxic heavy metal ions, due to ZnO is highly sensitivity and surface area, but low stable and MgO highly stable and sensitivity, but lower surface area compared ZnO. Under the optimized conditions, this electrode exhibited good analytical performance determining for cadmium (Cd(II)) and lead (Pb(II)) levels. Furthermore, the performance of the proposed electrode for Cd(II) and Pb(II) measurement in milk was examined in detail. This MCPEs, which are used as a working electrode in SVS experiments. It can be constructed from a homogenized paste consisting of graphite powder mixed with paraffin oil and MgO/ZnONPs using an agate mortar and pestle (ElMhammedi *et al*., 2009).

The aim of this study is to determine the level of the two toxic heavy metals (Pb and Cd) in cow milk collected from, Haramaya Woreda, around Haramaya University and Haramaya University dairy farm using MgO/ZnO CPE as working electrode and anodic stripping voltammetry.

Objectives of the study

General Objective

To prepare, characterize and develop a more sensitive MgO/ZnO nano composite modified carbon paste electrode for the determination of (Pb and Cd) in cow milk around Haramaya University.

Specific Objectives

- To Synthesize ZnO, MgO and MgO/ZnO nanocomposite using precipitation and hydrothermal methods
- To characterize ZnO, MgO and MgO/ZnO nano composite employing XRD, SEM, FTIR and Uv-vis.
- To construct carbon paste electrode and modified carbon paste electrode of ZnO, MgO NPs and MgO/ZnO nanocomposite.
- To characterize CPE, ZnO and MgO/ZnO CPE using cyclic voltammetry.
- Optimize parameters such as pH of the solution, deposition time, deposition potential, and concentration of Pb and Cd for the determination of these toxic heavy metals using MgO/ZnO/CPs electrode.
- To determine the concentration of Pb and Cd in cow milk obtained from Haramaya University dairy farm and around Haramaya University using MgO/ZnO/CPs electro de and anodic stripping voltammetry.

2. LITERATURE REVIEW

2.1. Environment and Toxic Heavy Metals Pollutions

The word environment is used broadly refer to everything that surrounds us. It is therefore, includes all living organisms as well as non-living things. The environmental instability or imbalance and disturbances can be caused either due to human activities such as agricultural, industrialization, urbanization, mining, and etc (Joseph, 2008). Environment polluted by nano degradable plastics, pesticide, toxic heavy metals and etc. From these, this paper focuses on toxicity of heavy metals. The term Heavy Metals refer to any metallic element that has a relatively high density and is toxic or poisonous at low concentration (Lenntech, 2004). Heavy Metals are a general collective term, which applies to the group of metals and metalloids with atomic density greater than 4 g/cm^3, or 5 times or more, greater than water (Hawks, 1997) and also Heavy Metals are defined as those elements with a specific density at least five times the specific gravity of water, Heavy Metals include Cadmium (Cd), Copper (Cu), Lead (Pb), Zinc (Zn), Mercury (Hg), Arsenic (As), Silver (Ag), Chromium (Cr), Iron (Fe) and Platinum group elements, Copper and Zinc are essential trace elements for living organisms at low concentration (<10 mg/L). However, they become toxic at high concentration (>10 mg/L). Most of these metal ion (Cd, Cu, Zn, Hg, As, Ag, Cr and Fe) can be released from the industries are in simple cationic forms (Volesky, 1995). The characteristics of heavy metals are described by (Wang 2005).Toxicity that can last for a long time in nature. Heavy Metals cannot be degraded including bio treatment and are very toxic even at low concentration (1.0-10.0 mg/L).

Heavy Metals are dangerous because they tend to bio accumulate. Bioaccumulation means an increase in the concentration of a chemical in a biological organism over time, compared to the chemicals concentration in the environment. Compound accumulate in living things any time they are taken up and stored faster than they are broken down (Metabolized) excreted (Tsoumbarist *et al.*,1994). The greatest demand for metal sequestration today comes from the need to immobilize the metals released to the environment or mobilized by and partially lost through human technological activities. It has been established that dissolved metals

(particularly heavy metals) escaping into the environment pose a serious health hazard. They accumulate in living tissues throughout the food chain, which has humans at its top, multiplying the danger. Thus, it is necessary to control emissions of heavy metals into the environment. Due to increase in the world population and development of industrial applications, environmental pollution problem became important. Communities produce both liquid and solid wastes. Heavy metals at higher concentrations they can lead to poisoning.

2.1.1. Lead as Pollutant

Lead is regarded as highly hazardous for plants, animals and particularly for microorganisms. The main sources of lead pollution in agriculture and plants are lead mines, fuel combustion, sewage sludge applications and farm yard manure. The maximum acceptable concentration for lead in food stuffs is around 1 mg/kg. Long-term exposure to lead can result in a buildup of lead in the body and severe symptoms. These include anemia, pale skin, a decrease handgrip strength, abdominal pain, nausea, vomiting and paralysis of the wrist joint. Prolonged exposure may also result in kidney damage. If the nervous system is affected, usually due to very high exposure, the resulting effects include severe headache, coma, delirium and death. Continued exposure can lead to decreased fertility and/or increased chance of miscarriage or birth defects (Dobrzanski *et al*., 2005).

A major use is the production of anti-knock compounds particularly tetraethyl lead, Pb $(C_2H_5)_4$ for addition to petrol. The exhausts from vehicles are a major source of the environmental contamination by lead. Lead is present in exhaust gases mainly as lead halides and oxides, but incomplete combustion results in about 10% of alkyl lead compounds also being present. Other source of lead emissions are copper and nickel smelters, iron and steel production. Estimates vary as to the importance of vehicle emissions as the sources of the lead contamination (Dobrzanski *et al*., 2005).

2.1.2. Cadmium as Pollutant

Cadmium is a toxic metal and can cause serious health problems. Recently attention has been focused on its availability in water, soil, milk, dietary products, medicinal plants, herbal drugs, etc. The most common sources for cadmium in soil and plants are phosphate

fertilizers, non-ferrous smelters, lead and zinc mines, sewage sludge application and combustion of fossil fuels (Mc Bride, 2003). Critical levels for cadmium in soil are between 3-5 mg/kg. This level, in most cases, it cannot cause toxic or excessive accumulation concentration in plants; the lowest level of the element concentration in plants that can cause crop yield reduction is between 5-30 mg/kg. Surprisingly, a small amount of cadmium was detected in the stem, leaves, and seeds of the plant sample collected from polluted areas. This may be due to the polluted air from the surrounding area (Ogabiela *et al*., 2010).

The major route of cadmium exposure for the general population is via food. An increase in soil Cadmium content generally results in an increase of plant uptake of Cadmium although some soil and plant factors may influence Cadmium accumulation by plants. Crops grown in Cadmium contaminated areas have been found to contain elevated Cadmium content compared with normal levels. Therefore, human Cadmium exposure via food in contaminated areas can be many times above normal intakes and lead to Cadmium toxicity (Ogabiela *et al*., 2010).

2.2. Toxic Heavy Metals Accumulation in Food

Heavy metal toxicity is one of the major current environment health problems and is potentially dangerous because of bio-accumulation through the food chain. Food such as cereal crops, vegetables and animal products are highly affected in neighboring cities, industrial plants and busy highways than in agricultural regions (Sathyamoorthy *et al*., 2016). Heavy metal poisoning could result, for instance, from drinking water contamination (e.g. through Lead pipes), high ambient air concentrations near emission sources, or intake via the food chain. Some of the major contaminations are due to toxic metals presence in the food as a part of human diet has irrecoverable effects (Samaghail Binghila *et al*., 2008).

Table1. Ranking of risks associated with various heavy metals in food.

Relative priority	High	Medium	Low
Environmental risk	Pb, Cd and Hg	Cr, Co, Cu, Ni and Zn	Al and Fe

World Health Organization (WHO) has established levels of metals in foods above optimum condition should not be consumed. For this reason the levels of trace metals in our food should be of much importance and concern to us.

2.3. Contamination of Toxic Heavy Metals in Milk

Increase in industrial and agricultural processes have resulted in increased concentration of toxic heavy metals in the air, water and soil. These metals are taken in by plants and consequently accumulate in their tissues. Animals that graze on such contaminated plants and drink from polluted waters also accumulate such metals in their tissues and milk if lactating (Yahaya *et al.,* 2010). A large amount of these metals taken in by plants and animals subsequently find their way into the food chain. According to (Sathyamoorthy *et al*., (2016) report the concentration of Pb and Cd in fodder samples neighboring cities and nearby busy roads was 102 to 382 mg/kg and 0.87 mg/kg respectively. It is above the tolerable limit of 30 mg/kg (Pb) and 0.5 mg/kg (Cd). This ever increasing pollution has given rise to concern on the intake of harmful metals in humans. Metals enter the human body through inhalation, ingestion or absorption through the skin (Ogabiela *et al*., 2010). The intake through ingestion depends on food habit.

The toxicity of metals depends on a number of factors: the particular metal in question, dose absorbed and the age of the person concerned. For instance, children are directly exposed to the effect because they absorb several times the percentage ingested compared to adults and even brief exposure may influence developmental processes (Samara and Richard, 2009). Lead, cadmium and mercury residue in milk are therefore of great concern because milk is largely consumed by infants and children. Although some metals are essential nutrients, have a variety of biochemical functions in all living organisms and important industrial uses, their potential toxicity to humans and animals is a source of concern. It is, therefore, necessary to monitor and control their levels in consumed food. The measurement of metal levels is helpful not only in ascertaining risk to human health but also in the assessment of environmental quality (Binghila *et al*., 2008). Many reports indicated heavy metals in milk and attributed the presence of these heavy metals in milk and dairy products to exposure of lactating cows to environmental pollution, consumption of contaminated feed stuffs and

water as well as the production process. Cow milk is a good source of both micro and macro elements in human diet and the location of the cows determine their concentration (Dobrzanski *et al*., 2005). The levels of lead and cadmium in milk from cows grazed on open fields in Kaduna were reported to exceeded the permissible maximum daily intake (0.05 mg/kg body weight) recommended by WHO (Lawal *et al*., 2006).

2.4. Biochemistry of Toxic Heavy Metals

The poisoning effects of heavy metals are due to their interference with the normal body biochemistry in the normal metabolic processes. When ingested, in the acid medium of the stomach, they are converted to their stable oxidation states and combine with the body's bio-molecules such as proteins and enzymes to form very stable bio- toxic compounds, which become difficult to be dissociated, due to their bio-stabilities, during extraction from the body by medical detoxification therapy. The equations below show their reactions during bond formation with the sulphydryl groups (-SH) of cysteine and sulphur atoms of methionine (-SCH_3).

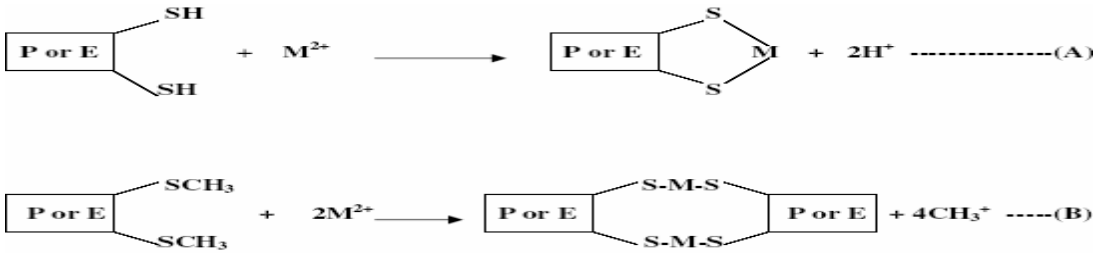

Where: (A) = Intermolecular bonding; (B) = Intermolecular bonding; P = Protein; E = Enzyme; M = Heavy Metal

The hydrogen atoms or the metal groups in the above case are replaced by the poisoning metal and the enzyme is thus inhibited from functioning, where as the protein–metal compound acts as a substrate and reacts with a metabolic enzyme (Sailu, 2014).

2.4.1. Toxicity Limit Value of Heavy Metals

It is known that not all heavy metals are of the same toxicity value. From the standpoint of health and sanitation, the maximum allowable levels of toxins in food have already been set by global health organizations such as FAO and WHO. The amounts of lead and cadmium in

milk have been determined to be 1000 ppb and 100 ppb, respectively (Risher and DeWoskin 1999). Some of their limit toxicity values are given in the following table.

Table 2. Toxicity Limit value (according to Bis) Indian standards, WHO and EPA

Heavy Metals	Bis Indian Standards (IS105000:1991)(mg L^{-1})	WHO (mg L^{-1})	EPA (mg L^{-1})
	Desirable limit	Permissible limits	
Zn	5.0	15	5.00
Cd	0.01	No relaxation	0.010
Pb	0.05	No relaxation	0.050
Cu	0.05	1.5	-

Where; EPA is Environmental Protection Agency

2.5. Method of Determining Toxic Heavy Metals in Milk

There are two methods for determination of toxic heavy metals, the spectroscopic methods and electrochemical methods. Some of the spectroscopic methods are listed in the following table.

2.5.1. Spectroscopic Methods

Table 3. Methods used for the concentration of toxic heavy metals

Electro analytical methods	Principles	Disadvantages	Reference
Spectrophotometry	Photons are absorbed by the sample, this absorptions reduces the intensity of the photons reaching at the detector	-each method varies in sensitivity depending on the spectrophotometric reagent. - not sensitive enough to determine low concentration	Tercier, W. and Buffle, 2005
Flame AAS	Measures the absorption of radiant energy produced by a special radiation source (lamp), by atoms in electronic state	-limited for solutions, less sensitivity, problems with refractory elements, relatively large sample quantities required (1-2mL)	Yang *et al*., 2006
Graphite Furnace AAS	Measures the absorption of radiant energy produced by a special radiation source (lamp), by atoms in electronic state	Expensive, high initial capital, low precision, low sample throughout, requires high level of operator skill	Tercier, W. and Buffle, 2005
ICP-AES	Measures the optical emission from excited atoms analyte ions are separated based on their mass to (m/z)	Complicated instrumentation, not suitable for onsite, interference arises when species has the same m/z	Tercier, W. and Buffle, 2005
X-ray Flour-Escence	Uses x-ray as primary excitation source	Less suitable for analysis of minor and trace elements	Tercier, W. and Buffle, 2005

Although a various number of sensitive and reliable analytical techniques such as optical and atomic flame spectrometry, neutron activation analysis, spark spectroscopy etc have been used for trace metal analysis (detection), factors such as the high cost of instrumentation, extensive sample preparation and limited selectivity, difficulty in analyzing low level concentration reduce the efficiency of these analytical techniques when they are applied to multi component trace analysis in complex sample matrices (Tercier *et al.*, 2005). In recent time electrochemical methods emerged for determination of heavy metals.

2.5.2. Electrochemical Methods

Stripping voltammetry technique can be used to make routine analytical determinations at the sub-ppm level, although this requires a high degree of care with regard to laboratory technique and sample handling. Analytes that can be determined by stripping voltammetry can also be determined by other analytical methods at higher concentrations (samples whose concentration exceeds 1 ppm), although the converse is not necessarily true since stripping method can detect analytes even at parts per billion (Tercier *et al.*, 2005).

Voltammetry is a wide spread electrochemical technique that is based on the measurement of the current response to an applied potential. Electrochemical methods, especially electrochemical stripping analysis (ESA), are widely recognized as a powerful tool for the simultaneous determination of multiple types of metal ion, because of the combination of an effective pre concentration step with advanced electrochemical measurements of the accumulated analytes (Economou , 2005). Stripping voltammetric techniques are the most important voltammetric techniques and are reviewed in the following sections.

2.5.2.1. Mercury electrodes

The performance of ASV is strongly influenced by the material of the working electrode. Traditionally, hanging mercury drop electrodes (HMDE) have been used, mainly because clean surfaces can be easily regenerated with a new mercury drop. Moreover, the potential window where mercury stays electro-inactive is very large, so that very electronegative metals can be detected. Despite being long known as an electrode, it is still used and upgraded. For example, Adam *et al.* (2005) have detected Cd^{2+} and Zn^{2+} with a phytochelatin

modified HMDE using ASV. However, HMDE present several drawbacks: metallic ions such as Hg, Au and Ag cannot be measured and the use of mercury electrodes is now severely rest ricted due to obvious toxicity considerations. Mercury thin film electrodes (MFEs) could be an alternative as less mercury is necessary. Nevertheless, the development of mercury free analytical systems is becoming inevitable.

2.5.2.2. Bismuth film electrodes

In 2011, bismuth-film electrodes (BFEs) were introduced as an alternative to mercury film electrodes (MFEs) (Wang *et al*., 2011) BFEs are prepared by plating thin bismuth films on suitable electrode materials. The main advantages of the BFEs are that they are environmentally friendly, since the toxicity of bismuth and bismuth ions is negligible, and their analytical properties are comparable to those of MFEs. Bismuth can be placed on the same substrate as mercury: glassy carbon, screen-printed carbon ink and gold have been successfully used. BFEs offers a better separation between inter metallic compounds than MFEs, e.g., Cd^{2+} and $Pb^{2+,}$ even if a large excess of Cu^{2+} are present. By co-deposition of bismuth and target metals on the glassy carbon or carbon fiber substrate, bismuth-film electrodes could be obtained for stripping voltammetric measurements of Cd^{2+}, Pb^{2+}, Tl^{3+}, and Zn^{2+} at mg/L level (Lin Cui *et al*., 2015). The main disadvantage of BFEs compared to MFEs is their lower potential window, particularly a more negative anodic limit due to the fact that bismuth is more easily oxidized than mercury. However, the cathodic limit potential is almost the same as MFEs. The pH of the sample solution strongly affects the useful potential window of BFEs. As expected, the most cathodic potential limit was achieved in basic media whereas the most anodic potential limit was achieved in very acidic media. The other drawback of BFEs has a serious limitation because of insufficient adhesion of the film to the electrode surface which causes degradation of the electrode.

2.5.2.3. Carbon paste electrode

Carbon materials are mercury free current conducting electrode materials, possessing some attractive features, has higher complication capacity than metals and has the ability to form strong covalent bonds with some surface modifiers. These properties make the carbon electrodes currently very widely used in electro analysis (Stozhko *et al*., 2008). Carbon

electrodes are used for various sensing and detection applications due to their broad potential window, low background current and low cost (Farghaly, 2004). The carbon surface is electrochemically inert over a wide range of potential and can absorb various compounds by nonspecific physical sorption and specific chemisorptions. One of the disadvantages of carbon electrodes is that electron transfer rate is slower comparing to metal electrodes. The electron transfer reactivity is strongly affected by the origin and history of the carbon surface (Chen *et al.*, 2009). Due to this factor it is better to modified carbon paste electrode.

2.5.2.4. Modified carbon paste electrode

Chemically modified carbon paste electrodes (MCPEs) are cheap, easy to make, and have a low background current, and so have been originally designed as an alternative to mercury electrode. Metallic or metal oxide nano particles have been successfully employed to modify CPEs for stripping analysis (Švancara *et al.*, 2009). However, the inherent disadvantages of CPEs such as low mechanical stability and reproducibility limit their practical application. Moreover, the use of nonconductive binders such as paraffin oil may weaken the electrochemical performance of CPEs (Lee *et al* 2007). Therefore, new electrode material developments are still needed to meet the growing demands for on-site monitoring of trace heavy metal ions.

The use of conductive solid materials as binders in CPEs to replace traditional binder systems shows promise to improve performance. Mineral oil, ionic liquid and molecular wires have been used to prepare CPEs with improved conductivity, high mechanical stability, and fast electron transfer rates, but mineral oil is the main source of heavy metals due to this not used for detection of heavy metals. Nanostructured materials are also candidates because of their large specific surface area, good biocompatibility, and ease of preparation. Nanomaterial, special inorganic Nanomaterials modified CPEs exhibit many favorable characteristics for electro analysis, including fast response, high sensitivity and selectivity (Lahiff *et al.*, 2010). Inorganic nanomaterials are benefiting from the basic advantages of regular structure, chemical and thermal stability, high surface reaction activity and catalytic efficiency, large surface-to-volume ratio and strong adsorption ability. Inorganic nanomaterials are often used for electrode modification, In particular, metals, metal oxide, carbon and silica based nano

materials are the most commonly used inorganic nanomaterials in electrochemical detection of heavy metal ions (Lin *et al*., 2015).

2.5.3.4.1. Metallic Nanoparticles

Early electro analytical methods frequently employed the hanging mercury drop and mercury film based electrodes Metallic nanostructure materials exhibit unique electrical, optical and catalytic properties. For the time being, by functionalizing metallic nanoparticles with small chemical and bio-molecules, various detection methods with high specificity have been designed for toxic heavy metal sensing to detect the toxic heavy metals, because of their wide cathodic potential range, high sensitivity and repeatability (Lin Cui *et al*., 2015). Recently, a nanocomposite of reduced grapheme oxide bismuth nanoparticles has been synthesized for sensitive detection of multiple heavy metals, in which the detection limits of 2.8, 0.55, 17 and 26 μg/ L are obtained for Cd^{2+},Pb^{2+}, Zn^{2+} and Cu^{2+}, respectively (Sahoo *et al*., 2013). Similar to bismuth, antimony nanoparticles have also been proven to be highly sensitive and reliable for trace analysis of heavy metals in conjunction with (ASV). Forexample,(Sahoo *et al*.,2003) prepared an antimony nanoparticles modified boron doped diamond electrode for simultaneous determination of Pb^{2+} and Cd^{2+} over the range of 50–500 mgL^{-1}. In addition, nanosized noble, bimetallic and transition metal particles modified electrodes have emerged for electrochemical analysis of heavy metals. By layer-by-layer assembly, multi-layer of Au nanoparticles (AuNPs) and bimetallic Au–Pt nanoparticles with low detection limit of 0.008 mg L^{-1} for Hg^{2+} (Lin *et al*., 2015).

2.5.2.4.2. Metal oxides

Nanostructured materials are also candidates because of their large specific surface area, good biocompatibility, and ease of preparation. Nanomaterial metal oxides such as ZnO, Fe_3O_4, NiO, SnO_2, ZrO_4, TiO_2, MgO and MnO_2 have also been widely used in the detection of heavy metals due to their interesting nano-morphological, functional biocompatible, non toxic and catalytic properties. These materials exhibit enhanced electron transfer kinetics and strong adsorption capability. For example, porous MgO nanoflower has been synthesized to fabricate heavy metal sensitive electrode. By combining with square wave anodic stripping

voltammetry (SWASV), the modified electrode exhibits excellent sensing performance for Pb^{2+} and Cd^{2+} with detection limits of 2.1 pM and 81 pM, respectively (Cui *et al*., 2015).

Yantasee *et al*., (2008) synthesized Fe_3O_4 nanoparticles to modify carbon electrodes for detection of Pb^{2+} in urine and simultaneous detection of Cu^{2+}, Pb^{2+}, Cd^{2+} and Ag^{+} in natural water. By combining the high absorptivity of Fe_3O_4 microspheres toward As^{3+} and the advantages of ionicliquid, Gao *et al.,* (2013) reported a disposable plat form for electrochemi cal detection of As^{3+} at 8×10^{-4}µg/L level in drinking water under nearly neutral condition.

Zinc oxide nanoparticles can be synthesized by hydrothermal method have investigated the removal of Cd(II) and other heavy metal ions from aqueous solution by good removal efficiency of Cd(II) metal ions. The adsorption equilibrium isotherms were best described by Langmuir isotherm model (regression coefficients, R^2 > 0.99). Langmuir maximum adsorption capacity was found to be 387 mg/g for Cd(II) at 303 K. The adsorption capacity was decreased with increasing of temperature because the adsorption process was exothermic (Yantasee *et al*., 2008). MgO/ZnO composite nanosheets were synthesized by a simple thermal evaporation method could be used as good materials for immobilization of enzyme for the fabrication of efficient H_2O_2 biosensor (Jianwei *et al*., 2015).

2.5.2.4.3. Nanocomposite

Nanocomposite is composites in which at least one of the phases shows dimensions in the nano meter range. Nanocomposite materials have emerged as suitable alternatives to overcome limitations of micro composites and monolithics, while posing preparation challen ges related to the control of elemental composition and stoichiometry in the nanocluster phase (Pedro *et al*., 2009). Nanocomposite is materials that incorporate nanosized particles into a matrix of standard material. The result of the addition of nanoparticles is a drastic improvement in properties that can include mechanical strength, toughness and electrical or thermal conductivity. Nanoparticles have an extremely high surface to volume ratio which dramatically changes their properties when compared with their bulk sized equivalents. It also changes the way in which the nanoparticles bond with the bulk material. The result is show that the composite can be many times improved with respect to the component parts (Pedro *et al*., 2009). Nanocomposite can be classified as ceramic matrix, metal matrix and

polymer matrix nanocomposite. In recent time a lot of nanocomposites materials can be synthesis and used from this some of them are listed in table 4.

2.6. Methods of Nanocomposite Synthesis

Nanocomposite can be synthesis by co-precipitation methods, sol-gel methods and hydrothermal methods.

2.6.1. Co-precipitation Method

The co-precipitation method is used for the synthesis of metal oxides nanoparticles, mixed metal or metal ceramics nano-composites, produces precipitate that are separated from solution. Inorganic salts are used as precursors, dissolved in water and other solvents to obtain homogenous solution of ions, and then these salts start precipitating as hydroxides or oxalates when the critical concentration of species is attained followed by nucleation and growth phases (Stankic *et al*., 2016). The size and shape of particles is greatly influenced by solution pH, temperature and concentration of salt. After precipitation, filtration and washing is done followed by calcination to convert hydroxide into oxides with a definite crystalline structure. Different types of metal nanocomposite materials synthesized using this approach is listed in Table 4. The precipitating medium usually employed includes NaOH, NH_3 or NH_4OH, Na_2CO_3 etc (Ambreen Lateef1 and Rabia Nazir, 2017). The use of surfactants is also a common practice to avoid agglomeration which also tampers the particle size of the composites obtained by this technique. The method offers the advantage of being low cost, simple, water based reaction, flexibility, mild reaction conditions and size control (Stankic *et al*., 2016).

2.6.2. Sol-Gel Method

Sol-gel method gained attention as a promising method for the synthesis of nanomaterials owing to their mild reaction conditions and building up the materials from molecular precursors leading to variation in materials and properties. The resulting product of sol-gel method is either films or colloidal powder. The sol-gel method has capability of producing micro and nanostructures. The size, shape and structure of final product are greatly

influenced by the reaction parameters (Ambreen Lateef1 and Rabia Nazir, 2017). The process involves the simple wet chemical reaction based on hydrolysis and condensation leading to formation of sol which through the process of aging results in formation of an integrated network as gel.

The sol–gel method is also very attractive for the synthesis of nanostructures containing more than one component, since the slow reaction kinetics allows good structural engineering of the final product. Another advantage is that the reactions are conducted at low temperatures or at room temperature. The sol–gel process involves inorganic precursors that undergo various chemical reactions, resulting in the formation of a three-dimensional molecular network. One of the most common routes is via hydrolysis and condensation of metal alkoxides to form larger metal oxide molecules that polymerize to form the coating. The sol–gel procedure allows coating of substrates with complex shapes on the nanometer to micrometer scale, which some commonly used coating procedures cannot achieve. The substrates include colloidal particles, organic/inorganic crystals, or even fibers and nanotubes (Chen *et al*., 2010). The range of materials prepared using this technique is outlined in Table 4.

2.6.3. Hydrothermal Method

The hydrothermal method involves the heterogeneous chemical reaction in a solvent (aqueous or non-aqueous) occurring above room temperature and at pressure more than 1atm in a closed system (Akhtar *et al*., 2008). To modify the size and properties the use of surfactants, capping agents, mineralizers is a common practice. The new trend is to use this technique in combination with microwave, sol-gel that can not only vary the physiochemical and structural properties of the materials but in addition to that can result in formation of single phased materials with enhanced stability (Ambreen Lateef1 and Rabia Nazir, 2017). Further just by altering the temperature, time and pressure of the reaction particle size, in Figure 4. The hydrothermal growth technique is promising for low cost and for scaling up the synthesis of nanostructures. This technique is not only useful to grow single material but can also be useful to synthesize nanohybrid or nanocomposite materials (Guo *et al*., 2011).

Table 4. Metal oxide nanocomposite (MONC) prepared from different approaches.

synthesize methods	MONC	Reaction condition	Particle size in (nm)	References
Co-precipitation	$MgO-Al_2O_3$	Centrifuged at 100 rpm	4-30	Nazari M. and Halladj R., 2014
	$ZnO-SnO_2$	pH 6, 105 °C	30	Ambreen and Rabia, 2017
	MgO-CuO	120 °C	20	,,
	$ZnO-Fe_3O_4$	pH 7, centrifuge	40	,,
	NiO. CeO. ZnO	120 °C	14-25	Stankic *et al*., 2016.
	Ag- AC	pH 8, N_2 atm	55	,,
	ZnO- AC	70 °C, pH 8	50-200	,,
Sol-gel method	TiO_2- Al_2O_3	-	5-9	Ambreen Lateef and Rabia Nazir, 2017.
	$TiO_2-Fe_3O_4$	100-1200 °C	4-10	Kundu *et al*., 1998.
	Al_2O_3-SiC	-	-	Yang *et al*., 2005.
	WO_3-TiO_2	Annealed at 550°C	-	Yang *et al*., 2005.
Hydrothermal Method	ZnO-kaolinate	Calinated 600 °C	14.6- 48.2	Stankic *et al*., 2016
	$Al_2O_3-TiO_2$	pH 8, 500 °C	3.25	Ambreen and Rabia , 2017
	$CdS-TiO_2$	160 °C	4- 6	Kundu *et al*., 1998.
	Co- MgO	150 °C	-	Karimi *et al*., 2011
	Ag- Graphene	-	-	Huang *et al*., 2012.

2.7. Preparation of Carbon Paste and Modified Carbon Paste Electrode

The CPE was prepared by thoroughly mixing 0.30 g of the graphite powder and 200 µL of paraffin oil using an agate mortar and pestle for 20 min until a visually uniform consistency.

The ILCP was prepared same way but using the IL. In case of the ILPCP, 100 µL of paraffin oil and 100µL of 1-methyl-3-octyl imidazolium bis(trifluoromethylsufonyl) imide were added simultaneously. The resulting CPs was then transferred into separate glass vials, compacted and let to stand overnight. To prepare electrodes, small portion of a paste was taken out with polyethylene splinter and packed 3 mm deep in a Teflon tube with internal copper wire electrical contact. The CP working electrodes made this way were always gently polished over a white photocopy paper in order to generate fresh surfaces and rinsed with water prior to each experiment (Tesfaye *et al*., 2016).

Similar to the CPE modified CPE was prepared by using bismuth oxide nanoparticles and ionic liquid modified carbon paste electrode (BONPs-IL-CPE). The 0.49 g graphite powder, 0.49 g *n*-octylpyridinum hexafluorophosphate (OPFP) and 0.02 g BONPs were hand-mixed in a mortar and pestle for 30 min. A portion of the resulting paste was packed firmly into the electrode cavity (1.8 mm diameter) of a glass sleeve with a spatula. The electrode was heated in an oven to temperature higher than the melting point of OPFP. The electrode contact was established via a copper wire introduced into the back of the sample (Ping *et al*., 2012).

2.8. Determination of Toxic Heavy Metals using Carbon Paste Electrode

Carbon materials are mercury free current conducting electrode materials, possessing some attractive features, has higher complication capacity than metals and has the ability to form strong covalent bonds with some surface modifiers. These properties make the carbon electrodes currently very widely used in electro analysis (Sotho *et al*., 2008). Carbon electrodes are used for various sensing and detection applications due to their broad potential window, low background current and low cost. The carbon surface is electrochemically inerts over a wide range of potential and can absorb various compounds by nonspecific physical sop tion and specific chemisorptions, due to this unique properties used for determination of toxic heavy metals (Fergal, 2004). One of the disadvantages of carbon electrodes is that electron transfer rate is slower comparing to metal electrodes. The electron transfer reactivity is strongly affected by the origin and history of the carbon surface (Chen *et al.*, 2006). According to different report toxic heavy metals was determined by carbon paste and modified carbon paste electrode, from this some of them are listed in table 5.

In this paper a novel carbon composite electrode modified with magnesium oxide/zinc oxide nanocomposite (MgO/ZnONCs) and paraffin oil. Such a composite electrode brings new capabilities for electrochemical devices by combining the unique advantages of nanomaterial s with the characteristics of a bulk composite electrode. Under the optimized conditions, this electrode exhibited good analytical performance determining cadmium ion (Cd (II)) and lead ion (Pb (II)) levels.

Table 5. Toxic heavy metals detected using CPE and MCPE

Electrode	Metals detected	References
CPE	Pb, Cd, Zn and Cu	Fikadu, 2016.
Ni/Zn/Fe_2O_4/CPE	Hg and Cd	Abbas *et al*., 2015.
Graphene-oxide/CPE	Pb	Sylwia Smarzewska and Witold Ciesielski, 2015.
ILC/SiO_2/CPE	Cu	Saghiri *et al*., 2016.
Cr/CPE	Zn, Cd, Pb and Cu	Koudelkova *et al*., 2016.

2.9. Stripping Analysis

Stripping voltammetric (SV) methods are the most efficient electrochemical voltammetric techniques for trace metal analysis and have been receiving considerable attention and currently available. Over the last decade SV has evolved into a very versatile and powerful analytical technique and it is a very sensitive electrochemical technique for measuring trace metals (Wang, 2005). The unusually high sensitivity and selectivity are based on the fact that the analytes is accumulated before it is determined and that both accumulation and determinat ion are electrochemical whose progress can be controlled.Since the metals are pre concentrate d onto the electrode by factors of 100 to 1000, detection limits are lowered by 2-3 orders of magnitude compared to solution-phase voltammetric measurements (Wang, 2005). With minimal sample preparation, this method is routinely capable of identifying and quantifying trace components from 10^{-9} to 10^{-11} mol/L and in some cases even 10^{-12} mol/L with excellent

sensitivity and selectivity. This means that stripping methods are among the most sensitive instrumental analysis methods of all; they are also superior to other trace analysis techniques as regards the correctness of the measured values obtained(Wang, 2005).

2.9.1. Principles of Stripping Techniques

Voltammetry is an electrochemical technique in which the current measured and displayed as potential peak and the resulting current is proportional to the concentration of the analyte. Stripping analysis involves two step techniques, the deposition step and the stripping step. The first step involves the electrolytic deposition or accumulation of a small portion of the metal ions in solution onto the electrode surface of an inert electrode at a constant potential to preconcentrate metals. This preconcentration step can involve either an anodic or cathodic process (Wang, 2005). Accumulation always takes place at constant potential of the metal to be determined and is called accumulation potential at a working electrode and based on an oxidation or reduction process. The particular dissolved metals are reduced and deposited as a layer on the working electrode that is subsequently oxidized. During deposition (pre concentration), the metallic ions in a solution is concentrated by the electrode in their metallic form. The electrode is scanned linearly toward positive potentials (in ASV) so that the metals, one at a time, are stripped from the electrode and re-oxidized at a potential characteristic of each metal (Jia *et al.*, 2007).

The accumulation time depends on the concentration of the analyte in the sample solution and must be chosen in a way that the measuring signal remains linear throughout as large a concentration range as possible. The time at which the graph is started to be plotted is called quiescent time (quiet time). During this period the potential is still applied but the stirring is stopped for 90 sec prior to analysis (Jia *et al.*, 2007). The resulting analytical signal is the current generated during the anodic “stripping” step and the plot of current versus potential is called a voltammogram. The resulting current- voltage peaks can be compared with those in a calibration curve of standard solutions of known quantities of metal ions. In all these procedures; the analyte of interest is accumulated on a working electrode by controlled potential electrolysis, while the solution is stirred. After a short rest period (10 seconds), this preconcentration step is followed by the second step called the stripping step which involves the removal of the accumulated analyte (dissolution of the deposit) species from the working

electrode and is the real determination step. This step consists of the application of a voltage scan to the electrode that causes an electrolytic dissolution or stripping of the species on the working electrode (Jia *et al.*, 2007). During this stage, the analyte is oxidized and the current is measured in which the oxidation of elemental species is registered as peaks in the current signal at the potential at which species is being oxidized. This means that the deposited analyte is removed ("stripped") from the electrode by a potential scan and the resulting current peaks are used to determine the concentration of each analytic species in the sample. Thus, a detectable current is produced at the electrode surface following the oxidation or reduction of the analyte at a characteristic potential.

The position of a peak potential (E_p) is a characteristic of the given substance and thus it can be used for qualitative identification, whereas the peak current (i_p) is proportional to the concentration of the corresponding analyte in the test solution. By careful interpretation of the resulted peak shape from current–potential voltammogram recorded during the stripping step, important and desired analytical information is readily obtained. This analytical quantitative information can be obtained from the height or area of the stripping voltammetric peak. Since stripping curves/peaks for various analytes occur at characteristic potentials, hence several species can often be determined simultaneously. The following reactions takes place on the working and counter electrodes during deposition and stripping steps.

During deposition: Working electrode (cathode) reduction reaction is: $M^{2+} + 2e^- \rightarrow M^0$

where: M^{2+} represents a divalent metal cation

$Pb^{2+} + 2e^- \rightarrow Pb^0$

$Cd^{2+} + 2e^- \rightarrow Cd^0$

Counter electrode (anode) oxidation reaction is: $2H_2O + 2e^- \rightarrow 4H^+ + O_2$

During Stripping

Working Electrode (anode), Oxidation reaction is: $M^0 \rightarrow M^{2+} + 2e^-$

$Pb^0 \rightarrow Pb^{2+} + 2e^-$

$Cd^0 \rightarrow Cd^{2+} + 2e^-$

Counter Electrode (cathode), reduction reaction is: $H^+ + 2e^- \rightarrow H_2$

Generally, stripping voltammetry analysis needs the followings four basic conditions.

Cleaning: - the potential is held at oxidize state greater than that of the analyte for a period of time to remove it from the electrode.

Potential held at a lower potential: - the potential of the system is held sufficiently low enough to reduce the analyte and deposit on the electrode.

Deposited material spread evenly on electrode: - if solid inert electrode is used this step not needed but must while using carbon paste electrode in the case of this study.

Working electrode is raised to a higher potential and stripping (oxidation) of the analyte.

The stripping may either be linear sweep stripping voltammetry (LSSV), Differential-pulse stripping voltammetry, Barker Square Wave Stripping Voltammetry and Osteryoung Square Wave Stripping Voltammetry. For time being the first two stripping technique are seen in detailed.

2.9.2. Differential Pulse Voltammetry

Differential-pulse stripping voltammetry is especially suitable because of its high speed and multi-element character. In this voltammetry, current is measured as a function of potential under conditions that encourage polarisation of the working electrode. For this purpose electrodes have a surface area in the range between a few square millimeters and a few square micrometers. Detection techniques of trace metals generally have high costs to be used in routine analysis (Silveira *et al*., 2013). However, differential pulse anodic stripping voltamme try (DPASV), has low operating costs and few structural requirements, besides having a scanning of "ppt" (parts per trillion).

2.9.3. Anodic Stripping Voltammetry

Anodic stripping voltammetry (ASV) is an extremely sensitive technique available for determination of trace metals and has the advantage of simultaneous determination of metals. Anodic stripping voltammetry (ASV) is used primarily for the determination of heavy metals (Jia *et al.*, 2007). In order to differentiate this method from other methods in which the determination does not take place by oxidation, but by reduction of the accumulated product, the term anodic stripping voltammetry (ASV) is used. In this case, the metals are preconcentrated by electro deposition onto the electrode surface. The preconcentration is done by cathodic deposition at a controlled time and potential. The metal ions reach the

electrode surface by diffusion and convection, where they are reduced and concentrated. The convective transport is achieved by electrode rotation or solution stirring. The duration of the deposition step is selected according to the concentration level of the metal ion. Following the preselected time of deposition, the forced convection is stopped and the potential is scanned anodically (Jia *et al.,* 2007), either linearly or in a more sensitive potential-time (pulse) waveform that discriminates against the charging background current. During the anodic scan, the metals are re oxidized, stripped out from the electrode surface in an order that is a function of each metal standard potential. The voltammetric peak reflects the time dependant concentration gradient of the metal at the working electrode during the potential scan. Peak potential serves to identify the metals in the sample. The peak current depends upon various parameters of the deposition and stripping steps as well as on the characteristics of the metal ion and the electrode geometry and it is proportional to the concentration of the metal ions in the sample.

2.9.3. Electrodes in Anodic Stripping Voltammetry

The choice of electrode in voltammetry is of outmost importance. The selection for the electrodes depends on their electrochemical inertness over a broad potential window, high overvoltage towards hydrogen and oxygen evolution, low residual current, low ohmic resistance and the possibility of a sufficiently simple surface regeneration. In anodic stripping voltammetry, a convectional three-electrode cell arrangement working electrode, reference electrode and counter electrode coupled to a computer desk top controlled by a soft ware is commonly used for anodic stripping voltammetric measurements (Farghaly, 2004). The working electrode, which makes contact with the analyte, must apply the desired potential in a controlled way and facilitate the transfer of charge to and from the analyte. It performs stripping, reduces the metal ions and deposits them on its surface of electrode in metallic form (Stozhko *et al*., 2008). During deposition, the working electrode acts as a cathode and reduces the metal ions to metal atoms. During stripping, a second electrode called the counter or auxiliary electrode becomes cathode and is used for the transfer of electric current to the test electrode and completes the other half of the electrochemical cell by hydrogen ions reduction to hydrogen gas and it must balance the charge added or removed by the working electrode. It is used to make connection to the electrolyte for the purpose of applying a

current to the working electrode. It does not take part in the reaction since they must be made of some inert material that prevent them dissolving in the electrolyte like mercury, graphite, gold or platinum. The third electrode is called the reference electrode which is a half-cell with a known reduction potential against which the potential is measured and is used to regulate the applied potential. Its only role is to act as reference in measuring and controlling the potential of the working electrode. The reference electrode must be stored in 0.1M KCl or NaCl when not in use to keep the tips wet so that its life time is extended. During this, the electrode was not entirely immersed in the solution or the pins kept dry since they may corrode or contaminated. These electrodes, the working, reference, and counter electrodes make up the modern three-electrode system in ASV as shown in the following Figure 1 (Stozhko *et al*., 2008).

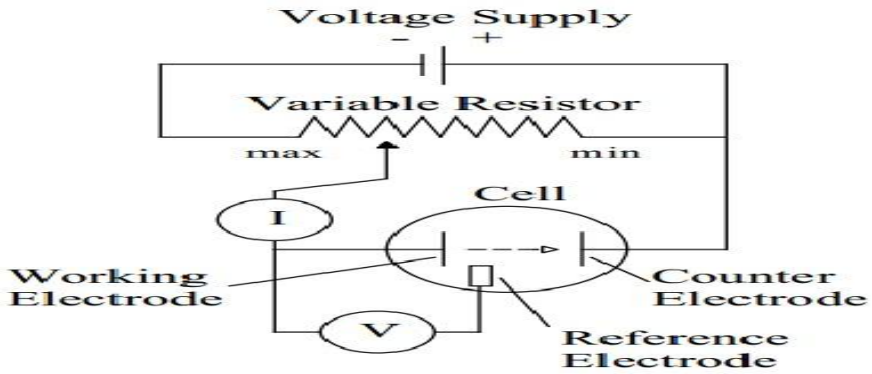

Figure 1. Three electrode systems used to carry out anodic stripping voltammetric experiments.

3. MATERIALS AND METHODS

3.1. Experimental Site

X-ray diffraction (XRD) and FT-IR analysis was conducted at Addis Ababa University and Scanning electron microscop (SEM) analysis was conducted at Leather Developemental Institute, Addis Ababa, Ethiopia. The synthesis of ZnO nanoparticles, MgO/ZnO nano composite and all other electrochemical characterization experiment were performed at Haramaya University, Chemistry Department Research Lab.

3.2. Instruments and Apparatus

The instruments used in this study were, pH meter (MP 220), furnace, XRD (BRUKER Advanced X Ray Powder Diffraction, AXS GmbH, Karisruh, West Germany). Scanning electron microscopy (SEM) (Mode-JEOL IT300) operated at 3kv with a special GC electrode. Bas100B Electrochemical Bioanalizer for all electrochemical measurements. A cell (10 mL), with three electrode configurations was used throughout the experiments with a modified GCE as working electrode, a platinum wire as auxiliary/ counter electrode, and an Ag/AgCl (satd. 3 M KCl) electrode as reference electrode. The area of the working electrode is 0.07 cm^2 in all experiments. All the cell potentials were measured with respect to an Ag/AgCl [3 M KCl (sat)] reference electrode.

3.3. Reagents and Chemicals

Glacial acetic acid and 99.5%, from Blulux, India, Ethanol 99%, Sodium hydroxide (NaOH) 40 g/mol and 98% purity, from LOBAL chemie), Hydrochloric acid (HCl) and 99 % purity Blulux, India, $K_3Fe(CN)_6$ and 99% purity from CDH, New Delhi, graphite 99%, paraffin oil extra pure, from Switzerland, cow milk, potassium chloride 99 %, sodium acetate 98 %, Zinc nitrate and 98% purity, from Blulux Laboratories Ltd, India, $Mg(NO_3)_2.6H_2O$ and 99% purity, from BDH chemicals Ltd Poole England, $Pb(NO_3)_2$ and 99%, from BDH, England, $Cd(NO_3)_2.4H_2O$ and 99% purity, from E. Merck, Darmstadt. All chemicals are analytical grade and were used without further purification. All solutions were made up with deionized water.

3.4. Experimental Procedures

3.4.1. Synthesis of ZnO Nanoparticle

ZnO nanoparticle was prepared by a precipitation method (Lanje *et al*., 2013; Nehal *et al.,* 2015). Two solutions were prepared: Solution A (0.1 mol of [$Zn(NO_3)_2.6H_2O$]) was prepared by dissolving 29.747 g of Zinc nitrate hex hydrate [$Zn(NO_3)_2.6H_2O$] in 200 mL distilled and deionized water; and solution B (0.12 mol Na_2CO_3) was prepared by dissolving 12.719 g of sodium carbonate in 240 mL distilled water. After that, the precursor was prepared by adding solution A to solution B drop wise under vigorous stirring for 2 h. The precipitate resulting from the reaction between the two solutions was allowed to settle down for 24 h, filtered with 0.2 µm membrane filter (Whatman) and washed three times each with deionized water and ethanol. The precipitate was dried at 100 ^{0}C for 6 h to form precursor of ZnO. The precursor obtained, after drying, was calcined in air at 300 ^{0}C for 2 h in furnace to get the ZnO nanoparticle. The product was labeled as ZnO NPs.

3.4.2. Synthesis of MgO Nanocomposite

To prepare MgO nanoparticle, 18.5 g of Magnesium Nitrate and 10 g of Sodium Hydroxide were dissolved in 250 mL distilled water in two breakers separately. It was stirred for half an hour using magnetic stirrer. Then the sodium hydroxide solution was added in to magnesium nitrate solution drop by drop with burette at room temperature. After 30 minutes milky white color precipitate was formed. Subsequently, the sample was filtered and washed with deionized water and ethanol three times and dried in an oven at 100 ^{o}C for 8 h, collected white color magnesium oxide nanoparticles after drying. The precursor obtained, after drying, was calcined in air at 500 ^{0}C for 2 h in furnace to get the MgO nanoparticle. The product was labeled as MgO NPs.

3.4.2. Synthesis of MgO/ZnO Nanocomposite

MgO/ZnO nanocomposite (16:1) ratio was prepared by mixing, 32g of Mg $(NO_3)_2$.$6H_2O$ and 100 mLof 2M NaOH solution by dissolving 5g NaOH in deionized water in separate beakers and stirred vigorously for sufficient time (Jianwei *et al*., 2015; SowriBab *et al*., 2015). In the

next step, NaOH solution was slowly added to the Mg $(NO_3)_2$.$6H_2O$ aqueous solution droply along the walls of the beaker for 30 min. While stirred and temperature of the solution was maintained at 60 ^oC. To this solution one gram of the as prepared ZnO was added and stirring was continued for two more hours and age for four hours. Subsequently, the samples were filtered and washed with deionized water and ethanol three times and dried in an oven at 100 ^oC for 8 h. The dried samples were annealed in furnace at 600 ^oC and allowed to stay for one hour at each temperature.

3.4.3. Characterization of the as Synthesized Nanoparticles

3.4.3.1. X-ray power Diffraction and SEM

The particle size of ZnO and MgO nano particles and MgO/ZnO nano composite was analyzed using XRD, wavelength of the incident radiation (λ = 0.15405 nm). Morphology of the as-synthesized nano particles was analyzed using Scanning Electron Microscope (SEM) instrument using V= 0.1-20 KeV.

3.4.4. CPE and Modified CPE Electrode Preparation

An established method (Ping *et al*., 2011) was used to prepare the carbon paste electrode. Graphite powder 5gm and 1.38 mL of paraffin oil (4:1 w/w ratio) were mixed togethers in a mortar and pestle to get the paste. The paste was mixed until a homogeneous paste was obtained for 30 minutes. The prepared homogenized paste was taken and kept in glass tube (inner diameter of 3 mm and length of 7 cm) and then a copper wire was inserted to provide electrical contact. The surface of the electrode was renewed or a new electrode surface was obtained by removing 2 mm (from the surface) of electrode material and adding freshly made graphite paste to obtain a smooth and fresh electrode surface. Before use, the surface of the electrode was polished with paper card and used immediately.

The modified carbon paste electrode was prepared by hand-mixing of 2.01 g graphite powder, 0.66 g paraffin oil and 0.39 g MgO/ZnO NCPs in a mortar and pestle for 30 min. A portion of the resulting paste was packed firmly into the electrode cavity (3 mm diameter) of a glass sleeve with a spatula. Electrode contact was established via a copper wire introduced

into the back of the sample. For comparison, 2.01g of graphite powder, 0.66g of paraffin oil and 0.39 g MgO and ZnONPs, was prepared in a similar way. The working electrodes were polished using wet filter paper, then washed with distilled water and dried.

3.4.5. Cyclic Voltammetric characterization of $K_3Fe(CN)_6$ on GC ,CPE and MCPE

The voltammetric behavior of 2 mM $K_3Fe\ (CN)_6$ in 0.1M KCl on Glassy Carbon Electrode, CPE, ZnO NPs, MgO NPs and MgO/ZnO nano composite modified CPE was investigated using Cyclic voltammetric. Moreover, the various electrochemical parameters were recorded from the voltammetric different scan rates (10-100 mV/s). The effects of scan rate on peak potential on bare and modified carbon paste electrode were examined by increasing the scan rate from 10 to100 mV/s.

3.4.6. Standard Solution Preparation

In the process of preparing and determining standard solutions, deionized water was used throughout the experiments. All the equipments used were first kept for 2 days in 6 M HNO_3, after which they were cleaned with distilled water and 1 g/L or 1000 ppm of standard metal solutions of Pb(II) and Cd(II) were prepared as stock solution from the nitrates of the corresponding metals $Pb(NO_3)_2$ and $Cd(NO_3).4H_2O$, respectively. Two 100 mL volumetric flasks cleaned, labeled and half filled with deionised distilled water were made ready. Then 0.1599 g $Pb(NO_3)_2$ and 0.274 g $Cd(NO_3)_2.4H_2O$ were accurately measured using analytical balance and added to prepared 100 ml volumetric flasks. 1 mL concentrated HNO_3 was added to each of the two volumetric flasks for dissolving the metals sample. After the salts dissolved, the volumetric flasks were filled up to the mark with deionized water (Wenshu *et al*., 2016). Then a series of Cd and Pb solution was prepared using proper dilution factors.

3.4.7. Optimization of pH

The pH value of a sample solution is one of the most important variables controlling the adsorption of the metal ions on the electrode. For selecting the solution pH, the stripping sensitivity of each element and the buffer capability was in consideration. The influence of the pH on the anodic stripping peak currents of Pb and Cd was studied while measuring the

pH in the voltammetric cell in the range of 2 to 8 in a solution containing 0.1 M sodium acetate buffer prepared by dissolving 4.1 g of CH_3COONa and 2.875 mL of CH_3COOH in 500 mL of deionized water, then the pH was adjusted using 0.1M HCl and 0.1M NaOH solution in acidic and basic medium, respectively, and the anodic peak current was measured for selection of maximum peak current (Yoseph Bereket, 2009).

3.4.8. Optimization of the Deposition Time

The dependence of the different anodic stripping peak current of the metal ions on the accumulation time in the standard solution was examined at constant concentration, pH, scan rate and deposition potential of the metal ions in the range of 60 to 150 seconds (Rodrigues *et al*., 2014).

3.4.9. Optimization of the Deposition Potential

According to (Marcos *et al*., 2014), **t**he influence of the variation of the accumulation potential on the peak current was studied and examined over the range of -0.7 to -0.4 V for Pb and Cd in a standard solution.

3.4.10. Milk Sample Extraction

Cow milk was obtained from Haramaya University dairy farm and around Haramaya Town. The treatment was performed using an established method (Tokusoğlu *et al*., 2004). From the collected milk 6 mL of representative milk was added into 10 mL tubes and Centrifugated at 3000 rpm for 10 min and then the lipid phases were precipitated. The upper phase including lipids was removed. The lower layer containing the minerals was transferred into another tube, and 100 µL of concentrated hydrochloric acid (HCl) and 100 µL of glacial acetic acid were added. Then the mixture was centrifuged at 3000 rpm for 20 min. The supernatant was collected and filtered at a pore size of 0.22 µm. Before transferring to electrochemical cells, the pH of the obtained extract solutions was adjusted to 4.5 by using 0.1 M NaOH solution.

3.4.11. Anodic Stripping Measurement

The voltammetric detection procedure consisted of pre concentration (accumulation), cathodic electrolysis (deposition) and stripping (detection) steps. During pre concentration step, the electrode was immersed in a cell containing 10 mL of metal ion solution for about 2 minutes and stirred at 300 rpm. The electrode was then removed, rinsed with deionized distilled water and again immersed into the voltammetric cell containing metal solution to be analyzed. A negative potential (–0.9 V) was applied to the electrode at the deposition time. The stripping voltammetry was performed in the same cell by anodic stripping potential toward positive direction. After each measurement the electrode surface was renewed using polushing (Cao *et al*., 2007).

3.4.12. Method Detection Limit (MDL) and Validity Test

Seven replicate blank samples were analyzed following the same procedures that have been utilized for the milk sample. Each of the blank samples was analyzed for its Cd and Pb concentration. The standard deviations of five blanks were used for MDL.

$$MDL = 3\times\sigma/S$$

Because of the absent of certified reference material for the milk sample in the laboratory, the analysis was carried out, validity of the methods employed for the investigation was assured by spiking the samples with standard solution of known concentration of the Cd & Pb to be analyzed (Meseret *et al*., 2013). To check the efficiency of the procedure, appropriate volume of 1000 mg/L of Cd and Pb was spiked into the milk sample using volumetric flask and analyzed for their respective spiked of Cd and Pb by the same procedure of milk preparation and detection using ASV.

The percentage recovery of the sample was calculated using the following equation:

$$R\% = \frac{amount\ of\ analyte\ recoverd}{amount\ of\ analyte\ add}\times 100$$

4. RESULTS AND DISCUSSION

4.1. Uv-vis Absorption Spectra Analysis

The Uv/vis absorption spectra of the as- synthesized nanoparticles ZnO, MgO and MgO/ZnO nanocomposite were shown in Figure 2. Maximum aborption band was appeared at 375 nm, 305 nm and 311 nm for ZnO, MgO and MgO/ZnO respectively. The band gap energy of as synthesis nanoparticles was found in table 6. Band gap energy (Eg) of the as synthesized nanoparticles was calculated using the equation depicted below (El-Kemary *et al*., 2010).

$$\mathrm{Eg} = \frac{1240\ eV}{\lambda}$$

Where, Eg is band gap energy in electron volts and λ is maximum wavelength (nm) corresponding to absorption edge or from direct replotted spectra of $(\alpha hv)^{1/2}$ vs hv (commonly known as Tauc plot) where α adsorption coefficient and v light frequency (Megersa Feyissa, 2014). The band gap energy (Eg) of the ZnO, MgO and MgO/ZnO were obtained by extrapolating to zero a linear fit to a plot of $(\alpha hv)^{1/2}$ against hv (often referred to as a Tauc plot) and the band gap energies are 2.77, 3.0 and 2.74 eV respectively.

Table 6. Maximum absorbance wavelengths and band gaps of the synthesized nanoparticles

Samples	Absorbance	Maximum wavelength (nm)	Band gap (Eg) (eV)
ZnO	1.62	375	2.77
MgO	0.67	305	3.0
MgO/ZnO	0.54	311	2.87

The energy of the band gap could be thus estimated to be 2.87 eV for MgO/ZnO. It is reported that the composite of MgO and ZnO increases in the stability of the nanoclusters (Lakshmi *et al*., 2012). The energy band gap of the MgO/ZnO was in between ZnO and MgO, this is due to additive effect of nanoparticles of interband absorption moves to higher energy (i.e. suffers "a blue shift").

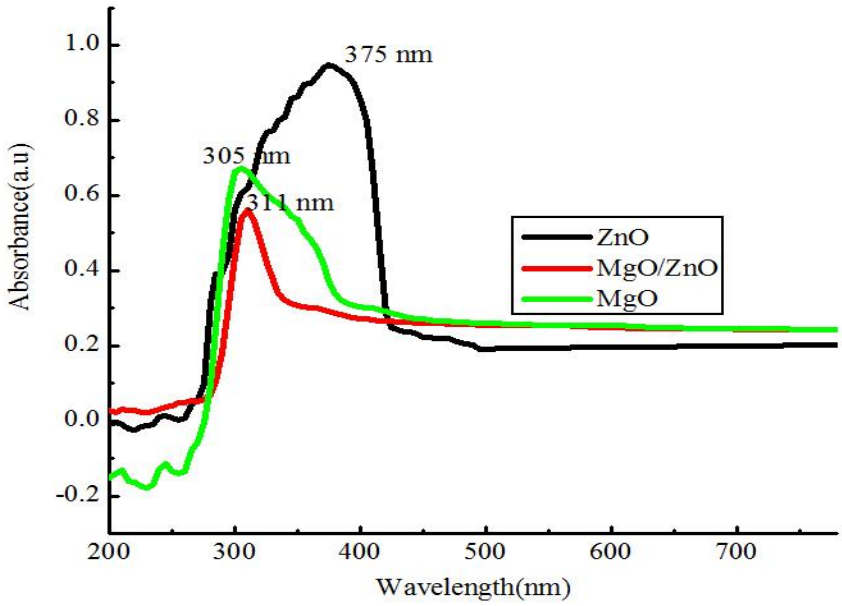

Figure 2. UV-Vis absorbtion spectra of ZnO, MgO nanoparticles and MgO/ZnO nanocomposite.

4.2. XRD Analysis

As a primary characterization tool for obtaining critical features such as crystal structure, crystallite size, and strain, x-ray diffraction patterns have been widely used in nanoparticle research. The x-ray diffraction pattern of ZnO, MgO and MgO/ZnO nanocomposite are shown in Figures 3. The results show distinct peaks with their corresponding 2θ and β values (given in units' degree and radians, respectively) which accounts for the crystalline nature of all the as-synthesized nanoparticles. The particle size (D) of the powders was calculated by Scherer's Formula;

$$D = \frac{K\lambda}{\beta \cos\theta} = \frac{0.90\lambda}{\beta \cos\theta}$$

Where, K = 0.90 is the Scherrer's constant, λ is the x-ray wavelength, θ is the Bragg's diffraction angle, 2θ is the angle between the incident and diffracted x-ray, and β is the peak width of the diffraction line at half of the maximum intensity. The average crystallite sizes of the as synthesized nanoparticles were calculated and listed in Table 7. From the table values the particle size of MgO/ZnO NCPs was smaller than MgO and ZnO. This indicates that the surface area of MgO/ZnO is higher than the rest, so the as synthesized nanocomposite was found to be highly sensitive towards heavy metals detection.

Table 7. Crystal size and energy band gap of the as synthesized nanoparticles

Sample	2θ (degree)	β (radians)	D (nm)
ZnO NPs	36.34	0.013	13
MgO NPs	43.22	0.0068	26
MgO/ZnO NPs	43.08	0.0158	11.3

The result is presented in Fig 3 a & b, the typical diffraction pattern and miller indices occurred at 31.8° (100), 34.4° (002), 36.3° (101), 47.5° (012), 56.6° (110), 62.9° (013) and 67.9° (112) for ZnO. In the other condition the typical diffraction pattern and miller indices of MgO at 38.28° (011), 43.22° (200), 48.28° (110) and 62.58° (202). Figure 3c shows that, clearly evidencing that the structure is composed of two crystalline phases, the strong diffraction peaks can be indexed as cubic MgO and the weak peaks occurred in the pattern should be related to the hexagonal like structured of ZnO. So that, the MgO/ZnO NCPs was composed of cubic and hexagonal structure with 11.3nm average particle size. This result is in agreement with (Jian *et al*., 2017).

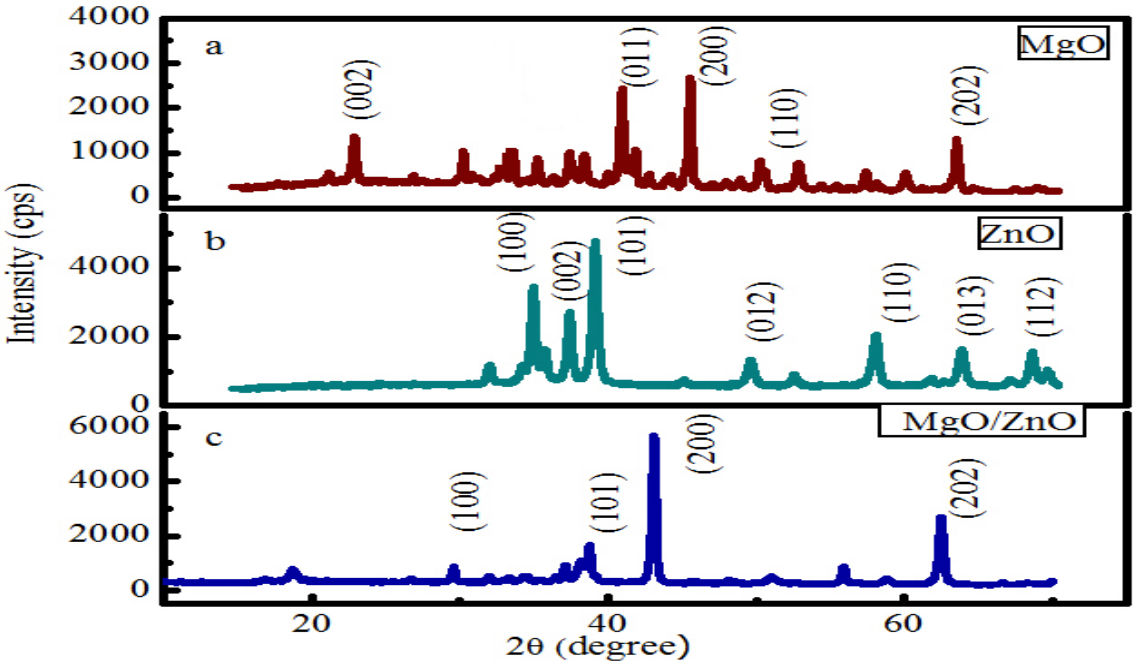

Figure 3. XRD pattern of MgO, ZnO nanoparticles and MgO/ZnO nanocomposite.

4.3. SEM and EDX Analysis

The SEM images of the as synthesized nanocomposite with selected magnification (×1000) are shown in Figure 4. The SEM image of ZnO nanostructures present a large number of nanosheet composed of hexagonal structure shown in (Figure 4b). In the case of MgO nanoparticles (Figure 4a) appears as inter-connected irregular and cubic structured. The binary MgO/ZnO nanocomposite SEM image (Figure 4c) shows that the uniform distribution of ZnO within the MgO/ZnO nanocomposite indicates the incorporation of ZnO into the irregular structure of MgO nanoparticles. The MgO/ZnO nanocomposite displays inter mixed features of nanosheet and irregular like structures due to irregular and nanosheet of MgO and ZnO nanoparticles. The energy dispersive x-ray spectroscopic analysis was for elemental composition present in the as synthesized nanopowders, performed coupled to a scanning electron microscope. It shows that (Figure 2a and 2b in appendix) the EDX data of MgO and ZnO NPs the elements magnesium and oxygen, and zinc and oxygen was observed with the atomic percent of metal to oxygen ratio of relatively one to one that confirms with the as-synthesized powder chemical composition. In other word (Figure 5c) shows the EDX spectra of MgO/ZnO nanocomposite, the signal of Zn, Mg and O elements clearly observed with the atomic ratio of 3, 40 and 53 %, respectively, in addition to this the atomic ratio of Mg to Zn is about (16:1). The impurities carbon and sodium was may be due to the precursor of Na_2CO_3 and NaOH used during synthesis of nanoparticles or metal oxide absorb CO_2 from air. This is similar result with (Haixia Chen *et al*., 2010). The atomic percentages of each element for the selected synthesized nano were behind the image of each figure 4.

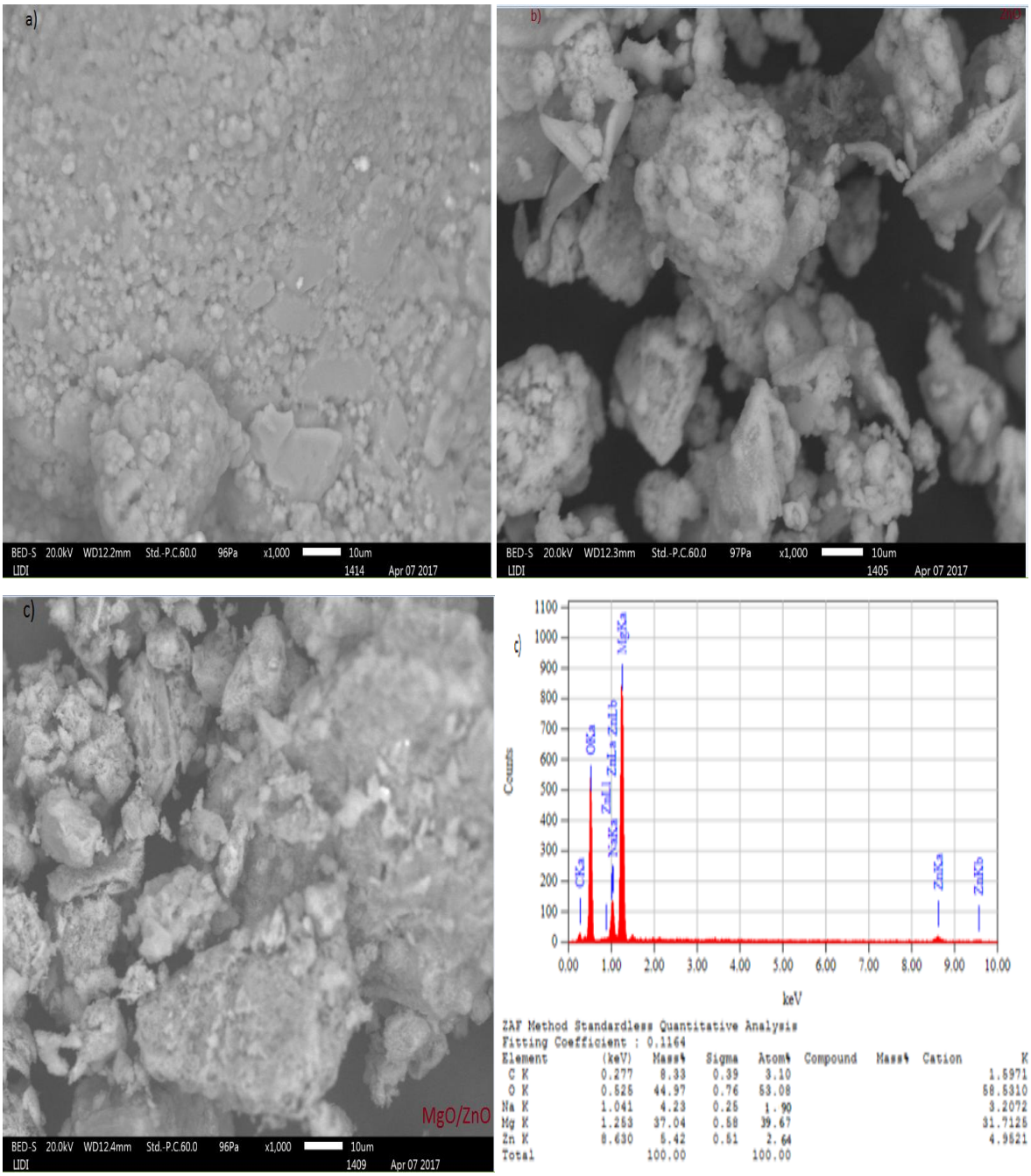

Figure 4. SEM images and EDX spectrum of a) MgO, b) ZnO and c) MgO/ZnO NCPs

4.4. FTIR Analysis

The FTIR spectra of MgO, ZnO and MgO/ZnO nanoparticles are shown in Figure 5. The broad band spectra around ~3445 and 3442 cm^{-1} (Figure 5) in the case of MgO, ZnO and MgO/ZnO corresponds to stretching mode of –OH group which may be due to the vibration mode of -OH group of adsorbed water molecule. These data are similar to the results

observed by others *(*Vennila *et al*., 2016). The absorption peaks in the region around ~1384 and 1563 cm^{-1} were also observed. Those absorption bands was due to vibrations of carbonates (absorbed CO_2 on the metallic cations). The presence of CO_2 molecules on ZnO, MgO nanoparticles were observed by infrared (IR) spectroscopy. The results revealed that the CO_2 impurities are formed by reactions involving the Na_2CO_3 precursors. The CO_2 is formed by thermal decomposition of zinc carbonate, which is a reaction product described below.

$$ZnCO_3 \rightarrow ZnO + CO_2.$$

These observations are in agreement with the model assumption that zinc carbonate is a source of CO_2 impurities; these data are similar to the results observed by others *(*Win, 2007). The absorption peak at ~ 835 and 534 cm^{-1}corresponds to Mg -O vibrations; these data results are agreed with the others (Vennila *et al.*, 2016). The band located around ~880 and 476 cm^{-1} can be attributed to the Zn-O stretching mode.

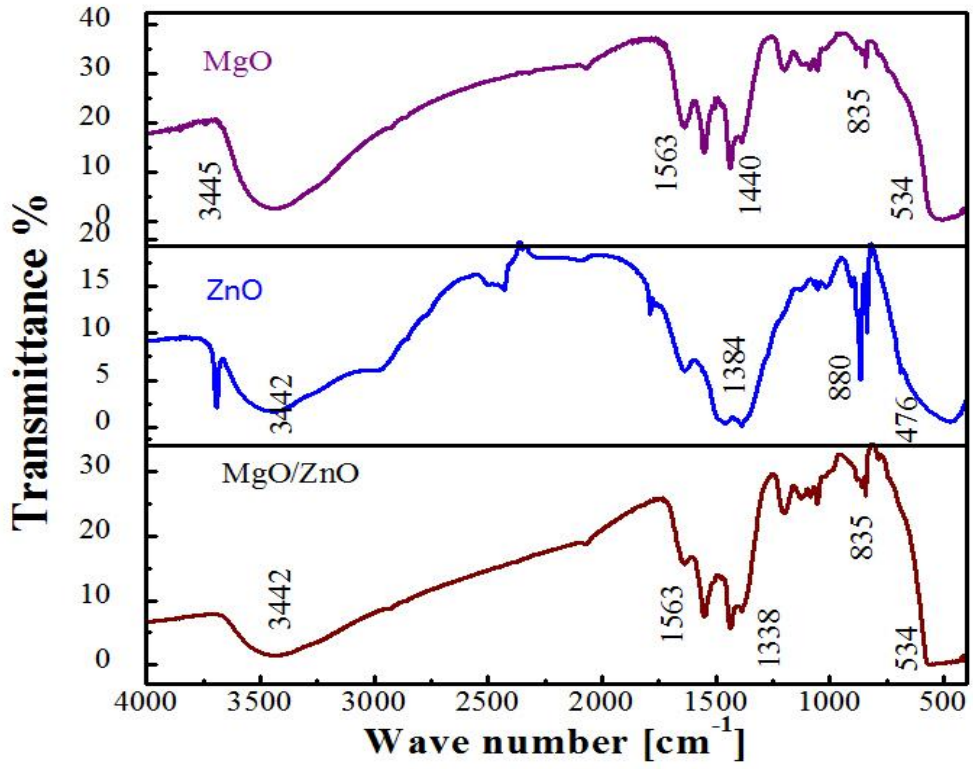

Figure **5**. FTIR Spectra of MgO, ZnO NPs and MgO/ZnO NCPs

These data are alike to the results observed by other similar reports (Viswanatha *et al.*, 2012*)*. The FT-IR result agreed with that of the EDX result, so the products are pure MgO/ZnO nanocomposite.

4.5. Electrochemical Characterization

4.5.1. Cyclic Voltammograms of $K_3Fe(CN)_6$ on CPE, ZnO, MgO and MgO/ZnO nanocomposite modified CPE

Potassium ferrocynide was used as a redox probe for the calibration of Ag/AgCl (3M KCl) reference electrode. Cyclic voltammograms of 2 mM $K_3Fe(CN)_6$) solution in 0.1M KCl on GCE electrode at different scan rates (10 to 100 mV/s) is shown in Fig 3 and electrochemical parameters are summarized in appendix Table 1. The data reveals 0.219 V as the redox potential of $K_3Fe(CN)_6$. Which was comparable to its literature value 0.256V. There was a slight variation about 0.037 V difference. Therefore in this thesis work all the measured potentials was adjusted to this value and unless otherwise stated all the potentials indicated in this work are reference to Ag/AgCl (3M KCl).

Figure (6a-d) shows the cyclic voltammogram of CPE and MCPE in 0.1M KCl at scan rate of 50 mV/s. Electrochemical potential window for bare CPE was from -1.4 to +1.5V likewise ZnO, MgO and ZnO/MgO nocomposite modified CPE. From fig (7a) shows the cyclic voltammetry curves of CPE, fig (4a-d) in the appendix indicate by plotting I_p *vs* $V^{1/2}$ graph and calculating the slope, the apparent diffusion coefficient of $K_3Fe(CN)_6$ was determined to be 7.6×10^{-6} cm^2s^{-1}. The linearity of anodic peak current *vs* square root of scan rate revealed that the diffusion of ions was controlled. The surface area of the CPE was determined by using Randles Sevcik equation:

$$Ip = 2.69 \times 10^5 n^{3/2} A D^{1/2} V^{1/2} C \quad (1)$$

Where i_p is peak current in ampere (A), A is area of CPE in cm^2, D is the diffusion coefficient in cm^2/s, V is sweep rate in V/s and C is the concentration of $K_3Fe(CN)6$ in mol/cm^3. From this the active surface area of the CPE was found to be 0.109 cm^2. The result is higher than the work of (Gulcemal *et al*., 2017), (0.0259 (± 0.0013) cm^2 and little difference with the work of (Harsha *et al*., 2017), 0.154 cm^2. From the above result to justify the prepared CPE was 1.6 fold of the area of GCE ($0.07cm^2$), so that the prepared CPE was used for the determination of toxic heavy metals.

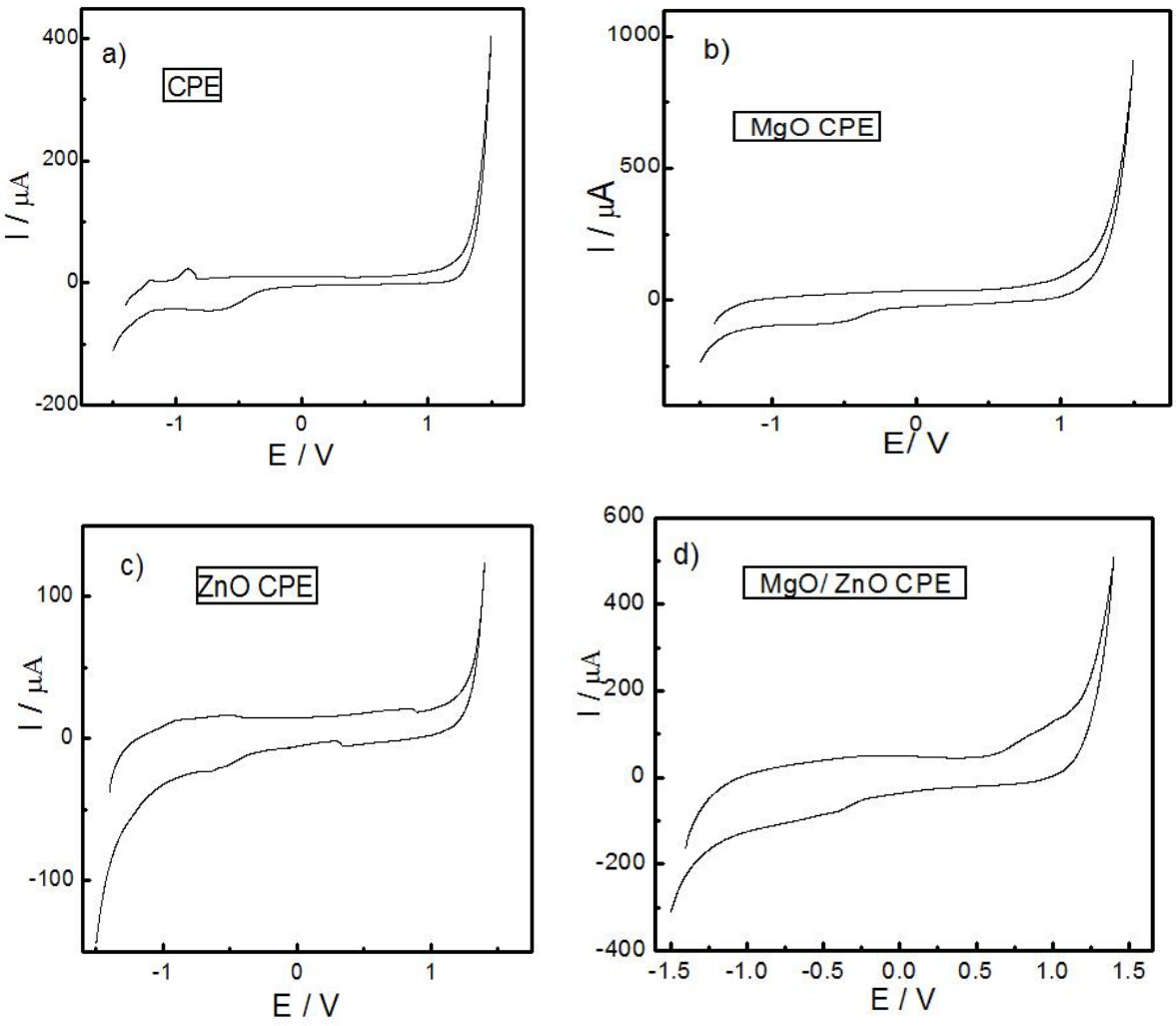

Figure 6**.** Potential windows of CPE a), MgO/CPE b), ZnO/CPE c) and MgO/ZnOCPE d) on CVs in 0.1 M KCl with Scan rate 50 mV/s

Electrochemical properties of CPE and MCPE was investigated using 2 mM $K_3Fe(CN)_6$ in 0.1M KCl as supporting electrolyte. Figure 7 shows cyclic voltammogram curves of ZnO, MgO, MgO/ZnO modified carbon paste electrode and CPE at different scan rate. On unmodified CPE (fig 7a) the peak current for potassium ferrocynide was lower in comparison to MCPE (fig 7e). ZnO/MgO binary system showed a better response for peak current as a result of synergetic effect increase surface area from the respective metal oxide nanoparticles On the other hand, the voltammetric response indicates a well manifested the oxidation and reduction peaks for $K_3Fe(CN)_6$. Moreover, the various electrochemical parameters recorded from the Voltammetric at different scan rates (10 to 100 mV/s) are summarized in Table 8.

As the scan rate increases the anodic and cathodic peaks potentials approximately/nearly cons tant and also the difference in anodic and cathodic peaks potentials falls in the range 81-115, 93-217, 90-167 and 77-145 mV for CPE, ZnO, MgO and MgO/ZnOCPE, respectively, this values was better than 302 mV, the work of (Fatima *et al*., 2017). As we seen from table 8 - 11, this process is reversible because the ratio of peak current found to be nearly 1. In other word the reversible process can be checked by heterogeneous electron transfer rate constant (k_s). The $k_s$values calculated from Laviron equation:

$$E_{pa} = E^{o'} + \frac{RT}{(1-\alpha)nF} + \frac{RT}{(1-\alpha)nF} \ln \nu \quad (2)$$

Where R=gas constant (8.314 J mol^{-1} K^{-1}), T = the room temperature (298.15 K), and F=the Faraday's constant (96484 C mol^{-1}), α = electrontransfer coefficient, n = number of electrons transferred in the redox reaction and v = scan rate (v /s). The αn value can be calculated for each electrode by using the slope of E_{pa}*v*s.ln*v* plot, the electron transfer rate constant can be calculated as follow:

$$k_s = \frac{\alpha n F v}{RF} \quad (3)$$

According to the above calculation all the electrode processes was reversible, because the value of the heterogeneous electron transfer rate constant (k_s) of CPE, ZnO, MgO and MgO/ZnO CPE was 1.39, 1.63, 2.08 and 2.8 respectively. This value is > 0.02 s^{-1} under the range of reversible reaction (Amani-Beni and Nezamzadeh-Ejhieh, 2017).

It is noted that the current corresponding to modified carbon paste electrode is higher than the bare CPE. Specially, the MgO/ZnO MCPE is excellent enhanced peak current, which is about two time's higher value when compared to bare CPE. This is mainly attributed to the higher active surface area of MgO/ZnO nanocomposite present on the surface of modified CPE, which implied that the electron transfer rate at MgO/ZnOCPE was significantly improved. The active surface area of ZnO, MgO and MgO/ZnOCPE was calculated from equation (1), the obtained value is 0.14, 0.162 and 0.186 cm^2 respectively. This is similar result in the case of ZrO_2/CPE (0.151cm^2) and ZrO2- GRP/CPE (0.225cm^2) (Harsha *et al*., 2017). The current response obtained for the modified electrode approves the effect of modifier in the electrode structure.

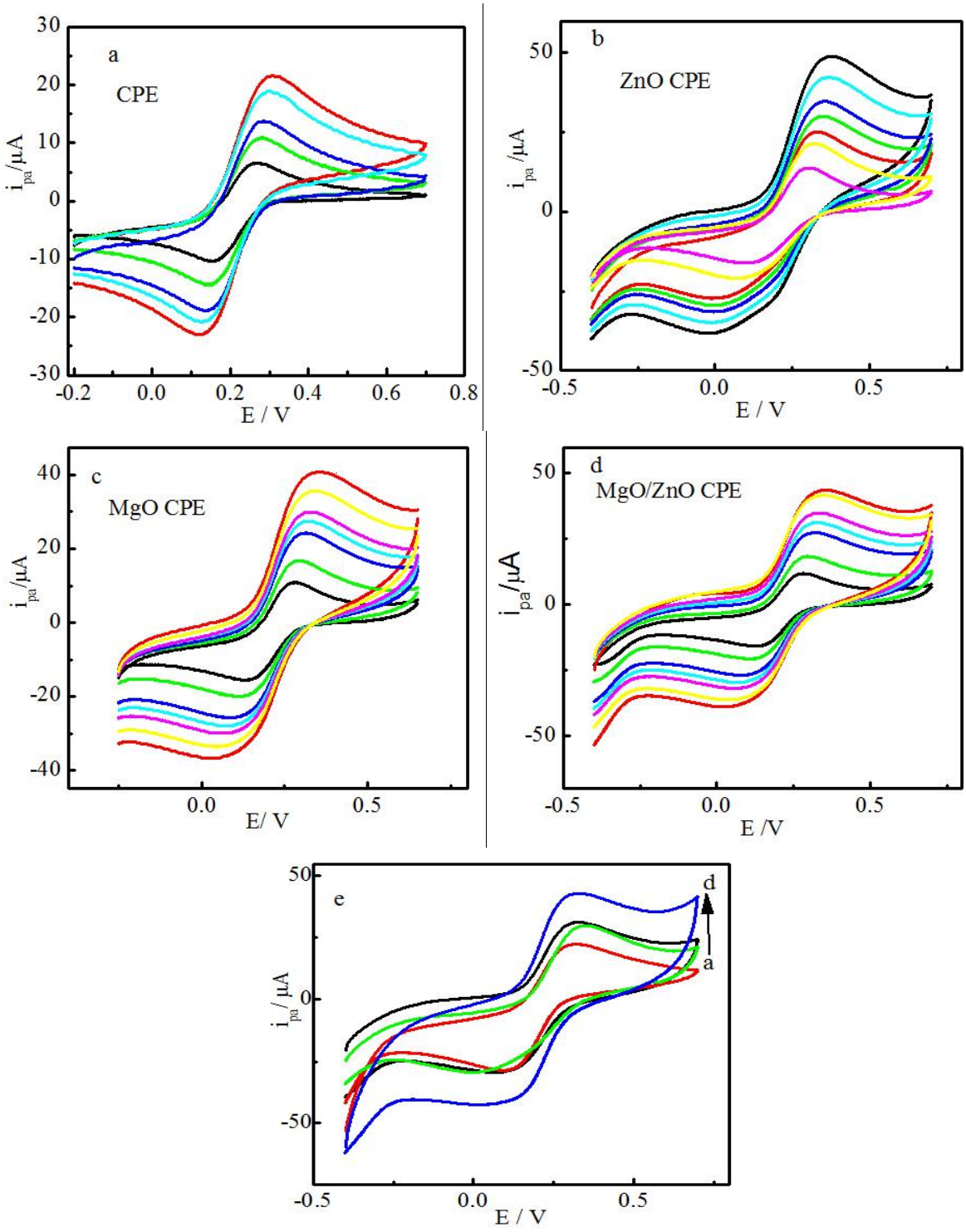

Figure 7. Cyclic voltammogram of 2 m M K_3Fe (CN)6 + 0.1 M KCl on a) CPE, b) ZnO, c) MgO and d) MgO/ZnO CPE at different scan rates 10, 20, 40, 50, 60, 80, 100 mVs^{-1}

Table 8.The effect of scan rate on peak current using CPE in 2 mM $K_3Fe(CN)_6$

Scan rate (mV/s)	i_{ap}(µA)	E_{pa} (mV)	i_{cp} (µA)	E_{pa} (mV)	i_{ap}/i_{cp}	ΔE_p (mV)
10	8.762	249	-10.3	168	0.85	81
25	12.999	262	-14.2	175	0.92	87
50	17.98	265	-18.07	167	0.995	98
75	18.91	269	-20.21	164	0.94	104
100	22.9	271	-23.02	154	0.995	115

Table 9.The effect of scan rate on peak current using ZnOCPE in 2 mM $K_3Fe(CN)_6$

Scan rate mV/s	$i_{pa\ (\mu A)}$	$E_{pa\ (mV)}$	$i_{pc\ (\mu A)}$	$E_{pc\ (mV)}$	i_{pa}/i_{pc}	ΔE_P (mV)
10	13.99	260	-15.71	168	0.89	93
20	20.79	267	-21.09	165	0.98	102
40	25.75	273	-26.05	150	0.99	123
50	29.86	286	-29.20	147	1.02	139
60	34.91	292	-30.92	139	1.13	153
80	42.69	316	-35.93	121	1.18	195
100	48.76	329	-39.03	112	1.23	217

Table 101.The effect of scan rate on peak current using MgOCPE in 2 mM $K_3Fe(CN)_6$

Scan rate m V/s	$i_{pa\ (\mu A)}$	$E_{pa\ (mV)}$	$i_{pc\ (\mu A)}$	$E_{pc\ (mV)}$	i_{pa}/i_{pc}	ΔE_P (mV)
10	10.78	262	-15.64	172	0.69	90
20	16.91	269	-19.95	164	0.85	105
40	24.05	272	-25.47	158	0.94	114
50	27.19	278	-27.79	155	0.98	123
60	29.99	284	-29.72	149	1.00	135
80	35.53	298	-33.59	142	1.05	156
100	40.58	305	-36.96	138	1.10	167

Table 11.The effect of scan rate on peak current using MgO/ZnOCPE in 2 mM $K_3Fe(CN)_6$

Scan rate m V/s	$i_{pa\ (\mu A)}$	$E_{pa\ (mV)}$	$i_{pc\ (\mu A)}$	$E_{pc\ (mV)}$	i_{pa}/i_{pc}	$\Delta E_P\,(\mathrm{mV})$
10	11.83	244	-15.68	167	0.75	77
20	18.31	247	-20.34	165	0.90	82
40	27.31	257	-27.16	163	1.00	94
50	30.08	260	-29.98	162	1.01	98
60	35.01	267	-32.76	156	1.07	112
80	41.13	275	-36.50	145	1.12	130
100	43.13	282	-39.04	137	1.13	145

4.6. Optimization of Experimental Parameters

In order to gain high sensitive electrochemical performance with CPE and modified ZnO, MgO and MgO/ZnO CPE to heavy metal ions, the effect of experimental parameters (pH, deposition time, concentration, and deposition potential) were discussed. Since buffer solutio n has the ability to fix pH value and ionic strength, therefore, it was widely employed as supp orting electrolyte in the practical analysis. Figure 8d (i) shows the stripping voltammograms i n 0.1 Msolutions of sodium acetate and acetic acid (NaAc-HAc) buffer, pH 4.5 to towards Cd (II) and Pb(II) on the MgO/ZnOCPE electrode. The back ground current responses of the CPE, ZnO, and MgO and ZnO/MgO modified carbon paste electrode (fig 8 i curves) and (fig 9 i curves), CPE modified with the MgO/ZnO (fig 8 and 9, curves), shows a larger response compare to others. This may due to improved surface area of the electrode outstanding to the presence of MgO and ZnO nanoparticles,

4.6.1. Effect of pH value of supporting electrolyte

Effect of pH value on the stripping peak currents was studied in 0.1 M acetate buffer with the pH range between 2 and 8 in the ASV and at 400 ppm metal ions. The result is shown in fig 8 and 9. The pH value influences the stripping peak currents and the maximum ASV peak wa s observed at the pH 4.5. The lower pH value result in a reduction peak current which was possible owed to the protonation of the hydrophilic groups reducing the absorption of metal ions (Huang *et al*., 2014). The peak current at the higher pH value above 5.0 was decreased,

which is possible due to the hydrolysis of Cd (II) and Pb (II). So, pH 4.5 was chosen as the optimal pH value for the analysis.

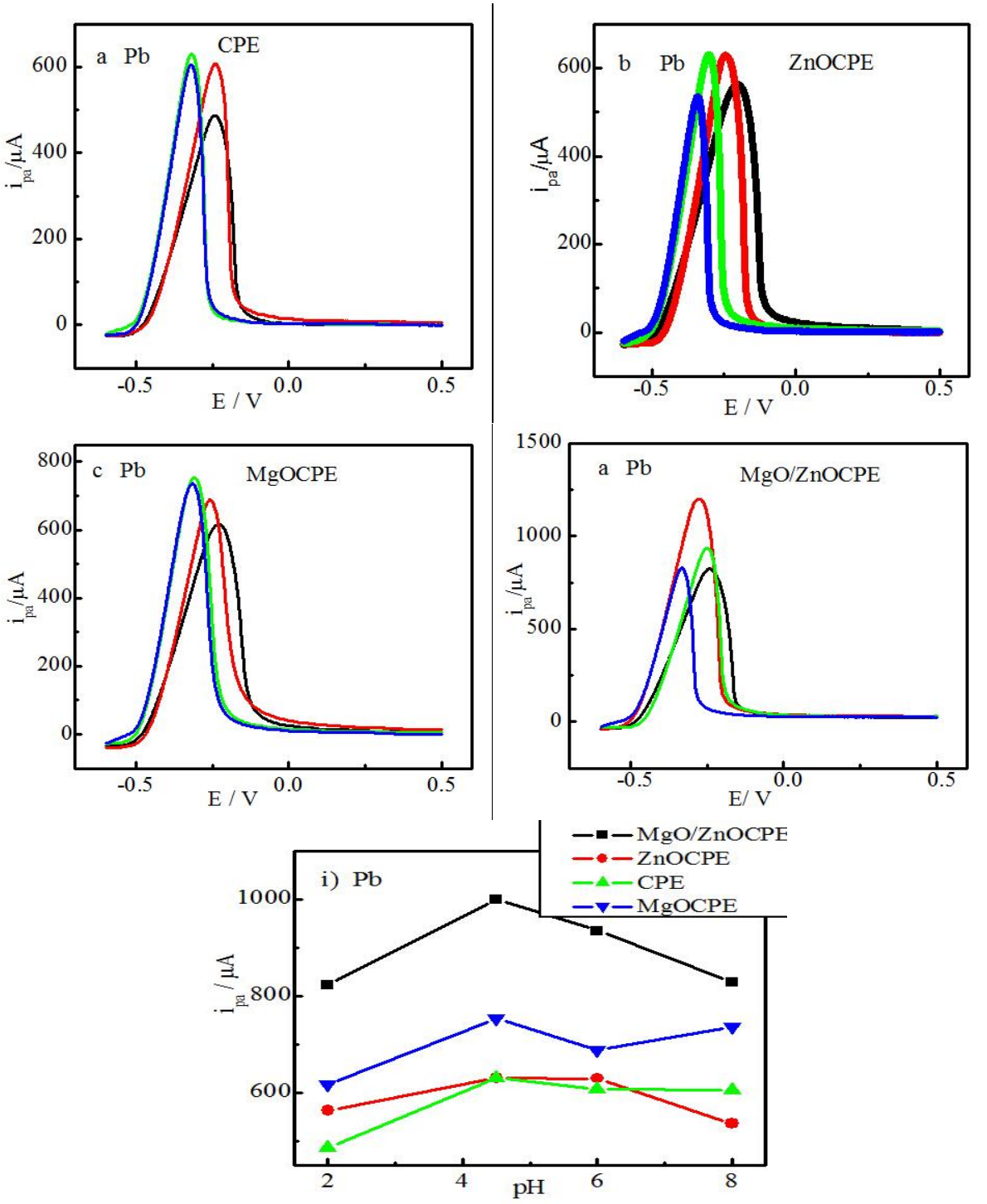

Figure 8. ASV of Pb ion at pH (2, 4.5, 6 and 8) with CPE and MCPE (a – d), and plot of peak current vs pH i & ii at constant deposition time 90 sec, concentration 400 ppm and at scan rate of 50 mV/s

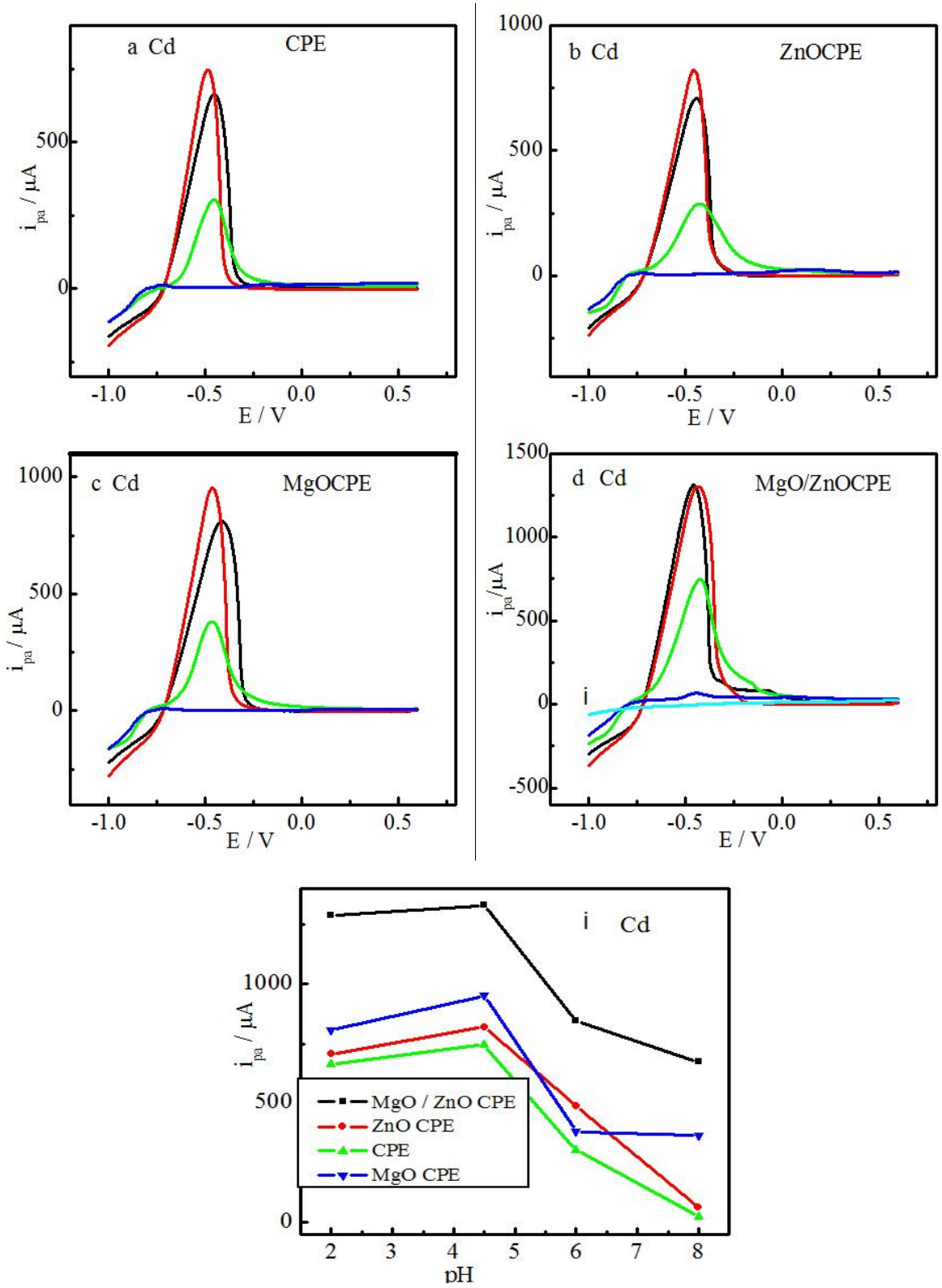

Figure 9.ASV of Cd ion at pH (2, 4.5, 6 and 8) with CPE and MCPE (a – d), and plot of peak current *vs* pH i & ii at constant deposition time 90 sec, concentration 400 ppm and at scan rate of 50 mV/s

4.6.2. Effect of Deposition Time

The deposition time effect on the anodic stripping peak current (I_{pa}) was studied in the range of 60-160 s at pH of 4.5 and concentration of 400 ppm for both Cd (II) and Pb (II) ion. It was found that, increasing the time required for deposition of cadmium and lead ions adsor bed on the electrode interface causes to increase discernibly the observed peak current at constant applied potential and scan rate of 50 mV *vs*. Ag/AgCl (fig 10). As it can be seen clearly in (fig 10 ia & ib), after elapsing 90s the observed peak current is independent from th e deposition time representing a restricted amount of the adsorbed Cd (II) and Pb (II) ion on the CPE and MCPE surface. In every case, the same behavior was observed, as the immersion time of the MCPEs in the solution containing the metal ions increases; the value of the anodic peak current also increases until reaching a limit value. According to article Álvarez *et al*., (2016) the limit value is the result of the equilibrium between the Me(II) ion that are adsorbed on the modifier and the Me^{2+} ions of the solution. It was noticed that the peak current reaches a limiting value depends on the modifier of the CPE and follows this descending order (fig ia&ib): MgO/ZnOCPE > MgOCPE > ZnOCPE > CPE; this order is consistent with the order corresponding to the active surface area of electrode mentioned in section (4.5.1). These results suggest that the larger surface area of the nanocomposite the greater the adsorption of Pb and Cd ion in agreement with XRD result. For this reason the deposition time of Pb and Cd metal ions was 90 seconds and all the subsequent experiments were performed within this deposition time besides, MgO/ZnO/CPE was selected for further experiments work.

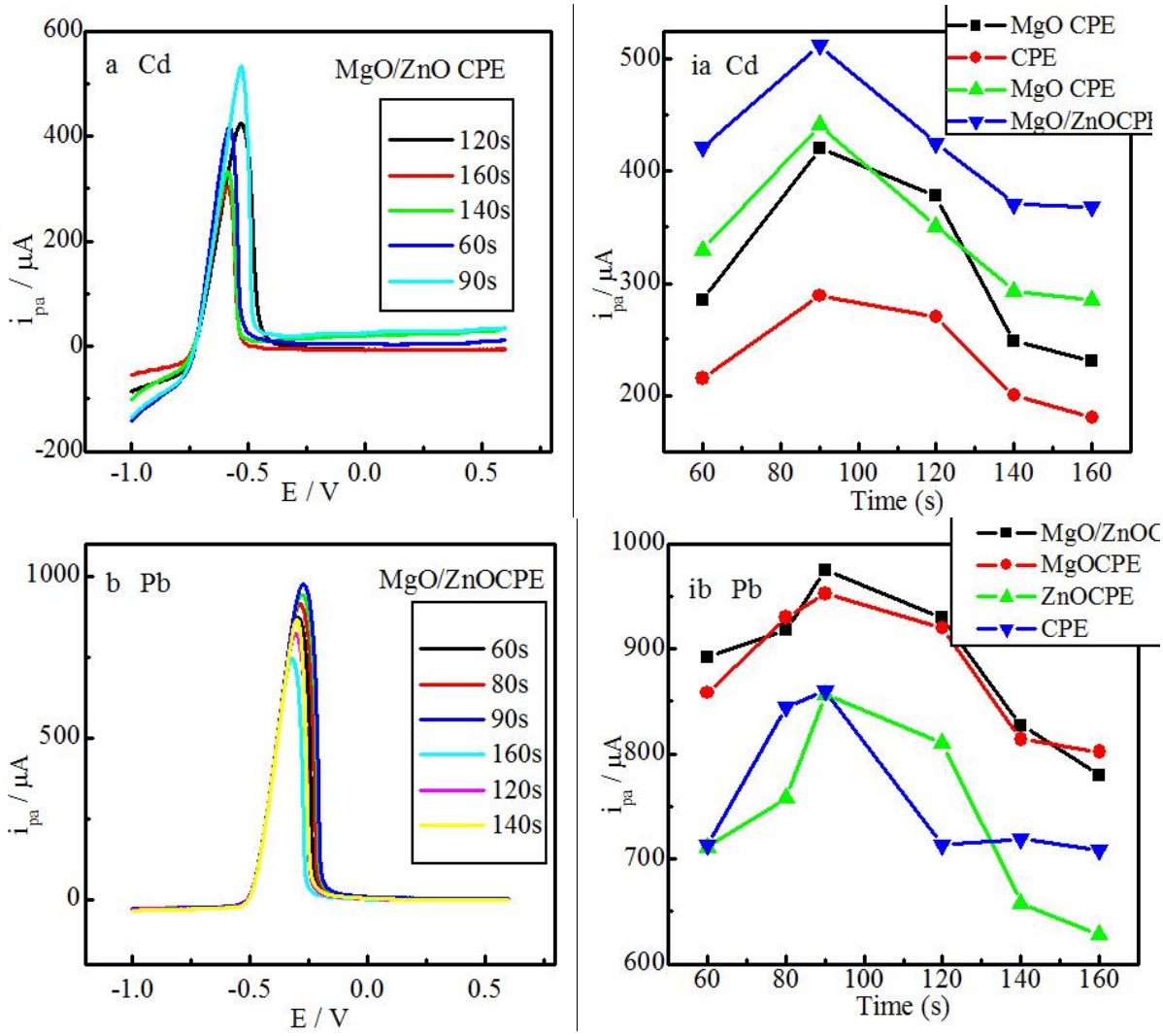

Figure 101. Anodic peak current verses time for Cd ia) and Pb ib) at different deposition time and current *vs* E for Cd,a) and Pb, b) at 0.1M acetate buffer pH 4.5, concentration 400 ppm and scan rate of 50mV/s.

4.6.3. Effect of Deposition Potential

The deposition potential of the analyte on the electrode's surface was evaluated by varying the potential from -0.9 to -0.4 V for Pb and -1 to -0.6V for Cd. Deposition potential is one of the essential experimental parameters which needs to be optimized before conducting the stripping voltammetric detection of an analyte such as Pb(II) and Cd(II) ions. Because as much as a proper potential to facilitate the reduction and deposition of the metal ions onto the surface of the electrode is not applied, the sensitivity of the electrode is greatly altered. Inorder

to reach the optimal stripping performance of the MgO/ZnOCPE the influence of deposition potential on the stripping signal for cadmium and lead is shown in fig 11(a & b) and a plot of peak current *versus* deposition potential is displated in fig11 (ia & ib). The more negative the deposition potential, the more easily Cd (II) and Pb(II) were reduced, thereby causing increase peak current. When the deposition potential become more negative, the reproducibility of stripping currents for Cd(II) and Pb(II) ions became poor, because hydrogen evolution was beginning to be significant in the medium at such negative potentials. Furthermore,the metals deposited on the electrodes surface might be damaged by the hydrogen bubble and lead to decrease in current signals at very negative potentials (Zhuo *et al*., 2017). Therefore, in order to obtain the high sensitivities, the deposition potential of -0.9 and -0.6 V was chosen for Cd(II) and Pb(II) ions respectively and these potentials were used for the detection of the two metals.

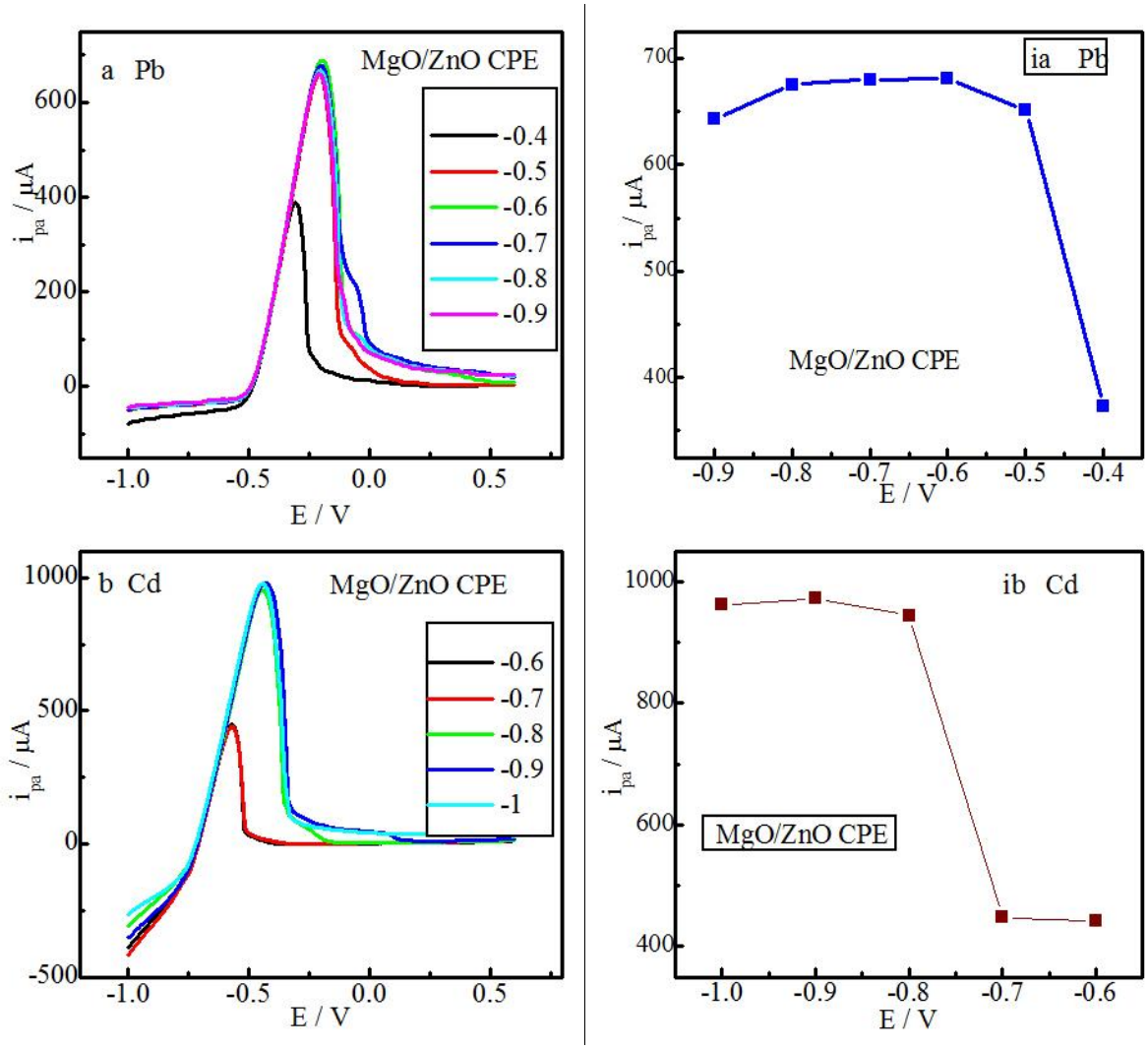

Figure 11. Anodic peak current *verses* different deposition potential at pH 4.5 acetate buffer, concentration 400 ppm, deposition time 90 sec and scan rate of 50 mV/s

4.6.4. Effect of Concentration

The performance of the CPE and MCPE as electrochemical sensor for the determination of Pb and Cd were evaluated by preparing a serious of Pb(II) and Cd(II) standard concentrations of 1, 100, 200, 300, 400, 600, 800 and 1000 ppm using anodic stripping voltammetry. The peak current of Pb(II) and Cd(II) increased with concentration up to 400ppm. Beyond 400 ppm, the peak current obtained was broad and reproducibility was poor but the peak was sharp up to 400 ppm for both metals fig 12 and 13. This fig shows the ASV responses of the CPE, ZnO, MgO and MgO/ZnO/CPE toward Cd(II) and Pb(II) at different concentrations. The corresponding calibration curve from 100 to 800ppm was:-

i_{pa} = 0.767x + 354.311 (R = 0.989), i_{pa} = 0.785x + 298.472 (R = 0.992), i_{pa} =0.787x + 434.472 (R= 0.996) and i_{pa} = 0.817x + 435.533 (R = 0.998) for Cd(II) and
i_{pa} = 0.721x +267.64 (R = 0.995), i_{pa} = 0.486x + 312.16 (R = 0.996) i_{pa} = 0.781x + 236.21 and i_{pa} = 0.7971x + 389.399 (R = 0.999) for Pb(II), with the order of CPE, ZnOCPE, MgOCPE, MgO/ZnOCPE, respe. Confirmation from the obtained results that the prepared elctrode is the most sensitive to selected Pb(II) and Cd(II) ions with good correlation co-efficient as we compeer with the singlet CPE and bare CPE shown on appendix fig 5. Therefore, for further and subsequent experiments, the concentration of the metal ions with 400 ppm was chosen.

4.6.5. Sensitivity and Limits of Detection

In order to evaluate the sensitivity of MgO/ZnOCPE electrochemical sensor, voltammograms were in the presence of different concentration of Cd^{2+} and Pb^{2+} was recorded. The result was as shown in fig 12 &13, anodic peak current increased with increasing of Cd^{2+} and Pb^{2+} concentration. The sensitivity, expressed as the slope of the linearly as concentration increases sensitivity also increases and the limit of detection (LOD) (based on a signal-to-noise ratio of 3 (S/N = 3) were found to be 0.45µg/L and 0.142µg/L for Cd(II) and Pb(II) ions respectively. This was compared with previously reported results, which was displayed in the Table 9. From the results it was confirmed that the electrochemically synthesized MgO/ZnO nanocomposite electrochemical sensor is highly sensitive to the detection of Cd^{2+} and Pb^{2+}. This is due to contribution of large surface area and higher current density.

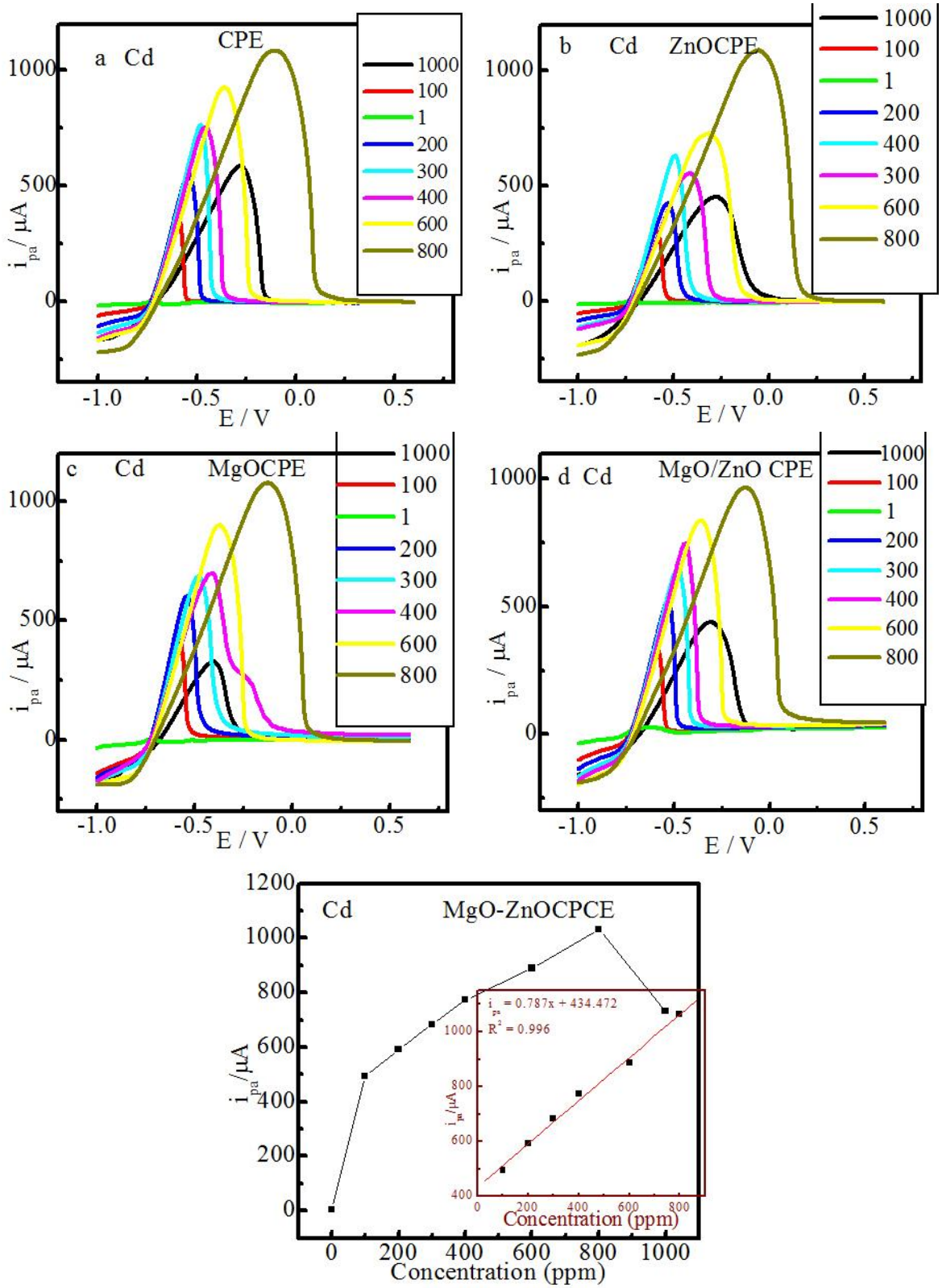

Figure 12. Plot of peak current *versus* concentration for Cd obtained from ASV at 0.1M acetate buffer pH 4.5, deposition time 90 sec and scan rate of 50mV/s

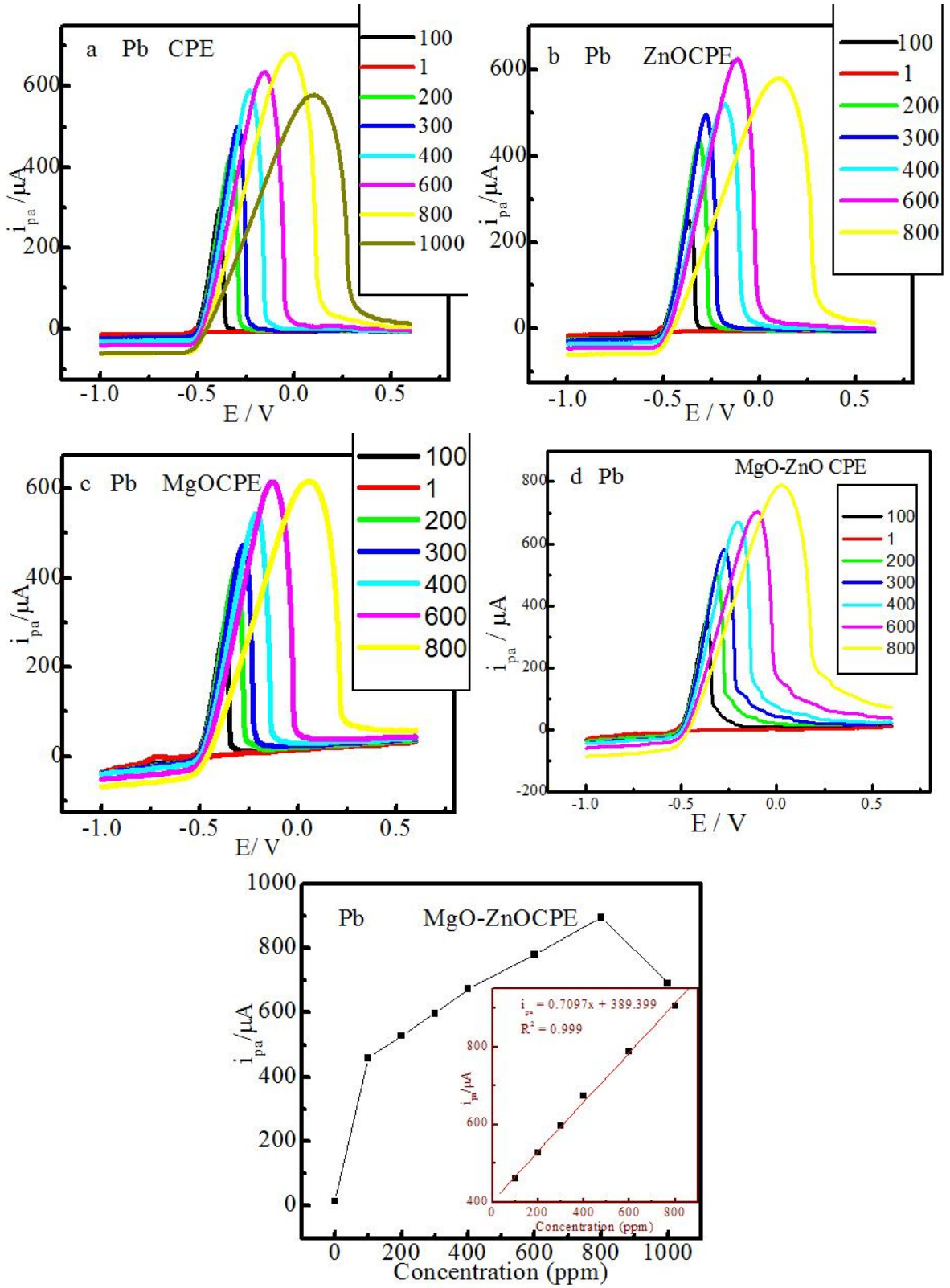

Figure 13. Plot of peak current versus concentration for Pb obtained from ASV at 0.1M acetate buffer pH 4.5, deposition time 90 sec and scan rate of 50mV/s

Table 12. The comparison this work with previously reported results

Modified electrode	Technique	LOD (µg/L)		Linear Range (µg/L)	Reference
		Cd	Pb		
Porous antimony film CPE	ASV	-	0.5	-	Ezzahra *et al*., 2017
Antimony(III) Salt CPE	SWASV	5	5	-	Švancara *et al*., 2010
SnO_2 quantum dots CPE	CV	499	-	4990 - 44910	Mahmoud *et al*., 2016
Graphene/polyaniline/poly styrene nanoporous CPE	ASV	4.3	-	10 -500	,,
Cr-CPE	SWASV	3	3	10 - 800	Koudelkova *et al*., 2017
RGO/Bi/CPE	DPASV	2.8	0.55	20 - 120	Zhuo *et al*., 2017
SbNP/MWCNT/CPE	SWASV	0.77	0.65	10 -60	,,
MgO/ZnO CPE	ASV	0.45	0.142	100 - 800	This work

4.6.6. Reproducibility and Stability of Modified Electrode

The storage stability and reproducibility of MgO/ZnOCPE were investigated by a series of repetitive experiment. After 3 weeks storage in dry state at ambient conditions, 99.5% of the initial current signal was retained, indicating that the prepared electrode had acceptable long-term stability. Secondly the repeatability MgO/ZnOCPEs was examined by performing three times at the same standard solutions 400 ppm Pb and Cd ions, the relative standard deviation (RSD), was 2.7%. For 5 successive measurements of metal ions (400ppm) with the same electrode shown in fig (14), RSD was 1.98%, which showing that the reproducibility was good. The long term stability and reproducibility of the MgO/ZnOCPEs make them attractive in the field of analytical applications.

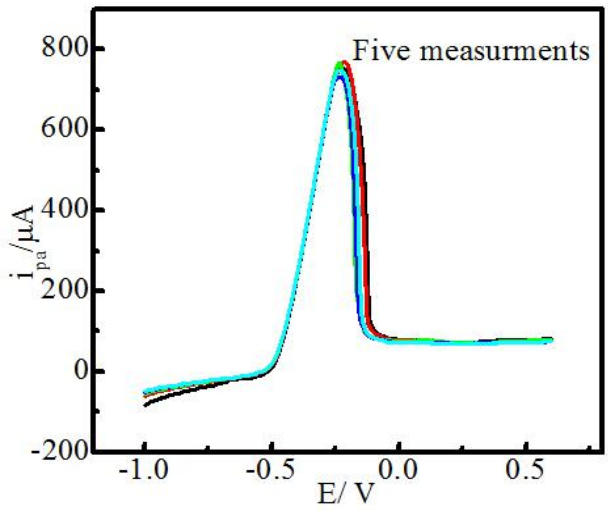

Figure 14. Anodic peak current *versus* potential of MgO/ZnO/CPE at 400 ppm detected by one electrode

4.6.7. Real Sample Analysis

In order to illustrate the application of ZnO/MgO/CPE sensor for the detection of Pb and Cd in real samples, milk obtained from Haramaya University dairy farm and from local farmars around Haramaya University was chosen. The determination of these two metal ions at the MgO/ZnO/CPE was performed by standard addition method. A typical analysis from these tests is shown in fig 15, the anodic stripping response of the prepared sample is shown with three consecutive standard additions of 400 ppm Cd(II) and Pb(II). The feasibility of the developed electrode for the determination of heavy metal ions in extracted milk sample was further examined by the recovery test. The results are summarized in Table 13. MgO/ZnO/ CPE possessed reasonable sensitivity and produced satisfactory recovery results with an average recovery of 100.0013% for Cd(II) and 100.0041% for Pb(II). The amount of both metals ions present in milk sample of Haramaya University dairy farm was 2.6 µg/L and 1.5 µg/L and sample that obtained around Haramaya University was 7.93 µg/L and 3.7 µg/L was less than the maximum allowed limits (0.02 and 0.01 mg/L for Pb and Cd) respectively (FAO/WHO, 1995). All of these results indicated that the fabricated modified MgO/ZnO/CPE sensor has a potential to be employed for the detection of trace heavy metal ions in environmental and food samples.

Table13.Recovery test for the determination of Cd(II) and Pb(II) in extracted milk samples

		Pb(II)			Cd(II)	
Sample name	Added(ppm)	Found (ppm)	Recovery%	Added(ppm)	Found (ppm)	Recovery%
Milk around HU	-	0.00793	-	-	0.0037	-
HU dairy farm	-	0.0026	-	-	0.0015	-
Milk around HU	400	400.00793 ± 0.0005	100.002	400	400.0037 ± 0.00125	100.0009
HU dairy farm	400	400.0026 ± 0.0008	100.0006	400	400.0015 ± 0.00067	100.0004

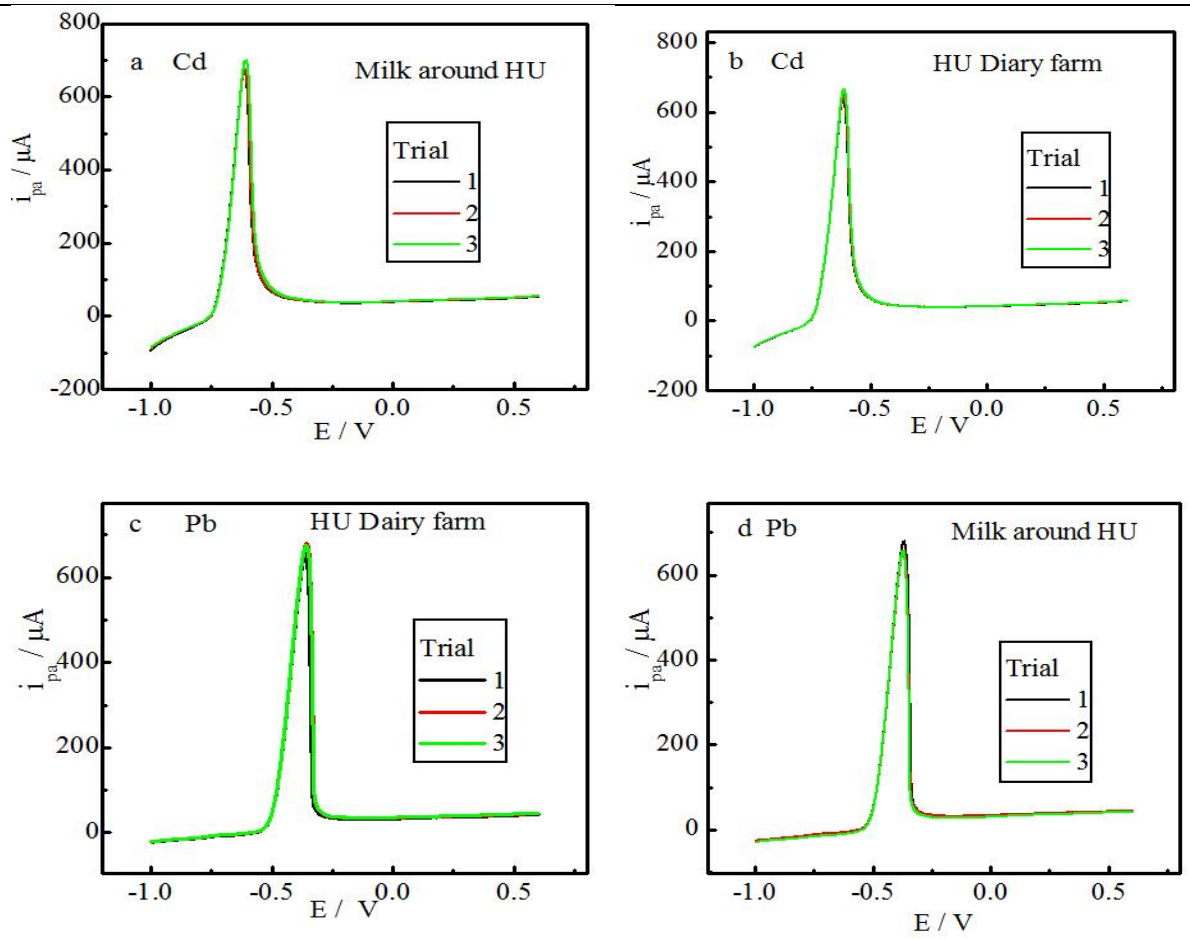

Figure 15. ASV of the extracted milk sample prepared after consecutive standard additions of 400 ppm Cd(II) and Pb(II) with 50 m V/s

4.6.8. Simultaneous Determination of Cd(II) and Pb(II)

As can be s seen from Figure 15, the voltammetric peak for the stripping of Cd(II) and Pb(II) using MgO/ZnOCE as a working electrode appears at different potentials with a separation of 290–630 mV between the stripping peaks, such a separation is large enough, and the simultaneous detection of Pb and Cd using MgO/ZnOCPE is feasible. There for the concent ration of Cd(II) and Pb(II) ions can be simultaneously determined.

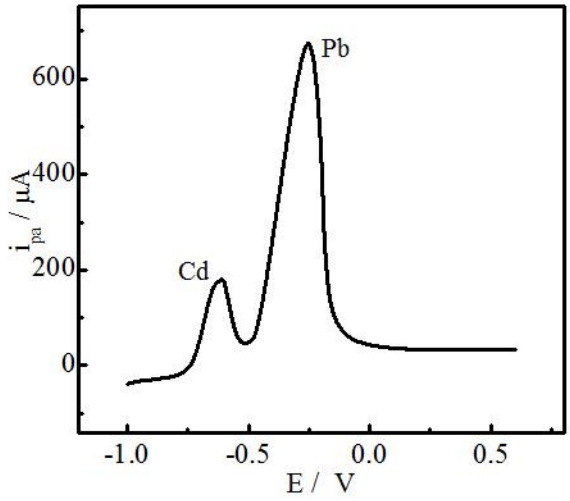

Figure 16. Simultaneous ASV response of Pb and Cd ions in milk sample by MgO/ZnOCE

5. SUMMARY, CONCLUSION AND RECOMMANDETION

5.1. Summary

In this work, MgO/ZnO nanocomposite has been successfully synthesized by hydrothermal method. The structural, functional and optical properties as well as morphological images of the synthesized products were characterized using the spectroscopic results of FT-IR, UV-Vis, XRD and SEM. From result of XRD the as synthesis nanocomposite was hexagonal nanosheet structure of ZnO and irregular structure of MgO with the average particle size of 11.3 nm. The SEM-EDX results also confirm the presence of both structures exhibited by the XRD. The electrochemical behaviors of MgO, ZnO and MgO/ZnO nanocomposite modified CPE was investigated using CV, the result showed binary modified CPE was more reversible, high surface area, low background current and excellent electrochemical properties. Besides, MgO/ZnO modified CPE was used for the determination of Cd and Pb under optimized condition in standard solution and in milk sample.

5.2 Conclusion

The amount of Pb and Cd ion present in the milk sample of Haramaya University dairy farm was 2.6 µg/L and 1.5 µg/L, where as sample that obtained around Haramaya University was 7.93 µg/L and 3.7 µg/L. This result was much lower than the guideline values in milk given by the WHO. Under optimized conditions the developed composite electrode exhibited a wide linear response range from 100 to 8000 ppm for both metal ions, and detection limit of 0.45 and 0.142 µg/L, stability 99.5%, average recovery above 100% for Cd(II) and Pb(II) respectively. In addition, the proposed electrode was applied to detect simultaneously trace metal ions in milk samples with satisfactory result of potential difference of 340 mV. Besides, stability, reproducibility and recovery of the MgO/ZnO/CPE were better than the single system modified CPE. Therefore MgO/ZnO/CPE can be applied for determination of Pb and Cd and holds great promise for wide application in environmental and food analysis.

5.3. Recommendations

Based on the findings of the present study, the following points are recommended.

- Synthesis MgO/ZnO/NCPs with different ratio is required to determine the best composition of the metal oxides and graphite and paraffin for toxic heavy metal electrochemical sensor application.
- It will be important to investigation the effect of binder such as ionic liquids for the prepare carbon paste and modified CPE to produce a more sensitive, selective and higher active surface area electrode
- In a future work, it is advised to use MgO/ZnO/CPE for other substances detection obtained from soil or industrial waste water.

6. REFERENCES

Abbas, A., Shadieh, S., Farzaneh, S., and Tayyebeh, M. 2015. $Ni_{0.5}Zn_{0.5}Fe_2O_4$ nanocomposite modified carbon paste electrode for highly sensitive and selective simultaneous electrochemical determination of trace amounts of mercury (II) and cadmium (II). *Journal of Iran Chemical Society*, 12:257–265.

Adam, V., Zehnalek, J., Petrlova, J., Potesil, D., Sures, B,. Trnkova, L., Kizek and Phytochela tin. 2005. Modified electrode surface as a sensitive heavy metal ion biosensor. *Sensor s*, *5*: 70–84.

Akhtar, M., Khan, M., Jeon, M. and Yang, O. 2008. Controlled synthesis of various ZnO nanostructured materials by capping agents-assisted hydrothermal method for dye-sensitized solar cells. *Electrochimical Acta*, 53(27): 7869-74.

Álvarez, Ignacio, G.M, Héctor, G. B., Lorenzo, G. O. and Juan, R. G. 2016. Modified Carbon Paste Electrodes Used to Evaluate the Retention Properties of Cd^{2+}, Pb^{2+} and Cu^{2+} on Biosolids, Soils and Biocomposites. *International Journal of Electrochemical Science*, 11: 2066 – 2084.

Amani-Beni, Z. and Nezamzadeh-Ejhieh, A. 2017. A novel non-enzymatic glucose sensor based on the modification of carbon paste electrode with CuO nanoflower: Designing the experiments by response surface methodology (RSM). *Journal of Colloid and Interface Science*, 504: 186–196.

Ambreen, L., and Rabia, N. 2017. Metal Nanocomposites:Synthesis, Characterization and their Applications. *Science and applications of Tailored Nanostructures*, 12: 239-256.

Brainina, K. Z., Stozhko, N.Y., Belysheva, O.V., Inzhevatova, L.I., Kolyadina, G., Cremisini, F. and Galletti, W. 2009. Determination of heavy metals in wines by anodic stripping voltammetry with thick-film modified electrode. *Analytical Chemistry Acta*, 514: 227-234.

Chaitanya L., Ananda, Somashekar and Ranganathaiah. 2012. Synthesis of ZnO/MgO Nanoc omposites by Electrochemical Method for Photocatalytic Degradation Kinetics of Eosin Yellow Dye. *International Journal of NanoScience and Nanotechnology*, 3(2): 47-63.

Chen, Q., Boothroyd, C., Soutar, A. and Zeng, X. 2010. Sol–gel nanocoating on commercial TiO_2 nanopowder using ultrasound. *Journal of sol-gel science and technology*, 53(1):115-20.

Chen, T.L., Wise, S.S., Kraus, K., Shaffiey, F., Levine, K., Thompson, D.W., Romano, B. and Wise, J.P. 2009. Particulate hexavalent chromium is cytotoxic and genotoxic to the North Atlantic right whale (Eubalaena glacialis) lung and skin fibroblasts. *Environmental Molecular Mutagenesis*, 50: 387–393.

Chuparina, E. V. and Aisueva, T. S. 2011. Determination of heavy metal levels in medicinal plant Hemerocallis minor Miller by X-ray fluorescence spectrometry. *Environmental Chemistry*, 9: 19–23.

Clara, P., Pedro, T., Núria, S., José M.D., Cristina, A., Miquel E. 2017. Determination of Pd(II) using an antimony film coated on a screen-printed electrode by adsorptive stripping voltammetry. *Talanta*, 167: 1–7.

Dobrzanski, Z.R., Kalaeu, H., Gorecka, K., Cholnaka, and Barkowalk, 2005. The content of micro elements and Trace Elements in Raw Milk from cows in Silesian Region. *Polish Journal of Environmental Studies*, 14 (5): 685-689.

Economou, A. 2005. Bismuthfilm electrodes: Recent developments and potentialities for electroanalysis. *Trends in Anal Chemistry*, 24: 334–340.

El-Kemary, M.H., El-Shamy and El-Mehasseb. 2010. Photocatalytic degradation ofciprofloxa cin drug in water using ZnO nanoparticles. *Journal of Alloys Compound*, 433:237-240.

ElMhammedi, M.A., Achak, M. and Chtaini, A. 2009. Modified carbon paste electrode for the determination of trace metals by square-wave voltammetry. *Journal of Hazardous Materials*, 161: 55-61.

Farghaly, O.A. 2004. A novel method for determination of heavy metals in water samples with mercury film-plated carbon paste electrode. *Talanta*, 63: 497-501.

Fatima, E. S., Aicha, O., Mama, E. 2017. Electrochemical detection of lead (II)atbismuth/ Poly (1,8-diaminonaphthalene) modified carbon paste electrode. *Arabian Journal of Chemistry*, 10: 596–603.

Fikadu, G., D. 2016. Anodic Stripping Voltammetric Determination of Toxic HeavyMetals (Pb, Cd, Zn and Cu) in Textile Effluent from Arbaminch Using Carbon Paste Electro de. MSc Graduate Project, Haramaya University, Haramaya, Ethiopia

Food and Nutrition Board, Institute of Medicine, 1997. Dietary Reference Intakes for calcium, phosphorus, magnesium, vitamin D and fluoride. National Academy Press, Washington. DC.

Food and Nutrition Board, Institute of Medicine, 2001. Dietary Reference Intakes for Vita min A, Vitamin K, Arsenic, Boron, Chromium, Copper, Iodine, Iron, Manganese, Molybdenum, Nickel, Silicon, Vanadium, and Zinc. National Academy Press, Washin gton, D.C.

Ganapathi, R., Ashok, K., Venkateswara, R., Shilpa, C. 2013. Structural properties of MgO Nanoparticles: Synthesized by Co-Precipitation Technique. *International Journal of Science and Research*, 4 (438): 43-46

Gao, C., Yu, X.Y., Xiong, S.Q., Liu, J.H. and Huang, X.J. 2013. Electrochemical sensing of heavy metal ions with inorganic,organic and bio-materials. *Journal of Analytical Chemistry*, 85: 2673–2680.

Guo, Z., Chen, X., Li, J., Liu, J.H. and X.-J. 2011. Huang, ZnO/CuO Hetero Hierarchical Nanotrees Array: Hydrothermal Preparation and Self-Cleaning Properties. *Journal of Langmuir*, 27: 6193-6200.

Haixia, C., Jijun, D. and Shuyi Ma. 2010. Structural and optical properties of ZnO:Mg thin films grown under different oxygen partial pressures. *Physical chemistry*, 42: 1487–1491.

Harsha, D., Deepak S. R. and Soami P. S. 2014. Black Rice Modified Carbon Paste Electrode for the Voltammetric Determination of Pb(II), Cd(II), Cu(II) and Zn(II). *Procection National Academic Science India A*, 84, 361–370. DOI 10.1007/s40010-013-0112-6

Harsha, D., Sana, A., Soami, P. S. and Rajeev, J. 2017. ZrO_2-Graphene-Chitosannanocompos ite modified carbon paste sensor for sensitive and selective determination of dopamin e. *Materials Today Chemistry*, 4: 17-25.

Huang, L., Jie, Z., Xuxian, X., Qiongqiong, H., Shun, L. and Fen, W. 2014. A Nonenzymatic Glucose Sensor Based on a Copper Nanoparticle Zinc OxideNanorod Array. *Analytic al Letters*, 47(7):1147- 1161.

Huang, L., Wang, Y., Tang J.,Wang, H., Wang, H., Qiu, J., Wang, Y., Liu, J. and Liu, J.2012. Synthesis of Graphene/Metal Nanocomposite Film with Good Dispersibility via Solvo thermal Method. *International Journal of electrochemical Science,* 7**:**11068 – 11075.

Huang, T., Chen, X., Liu and Ma. 2014. Ultrasensitive and simultaneous detection of heavy metal ions based on three dimensional grapheme carbon nanotubes hybrid elect rode materials. *Analytical Chemistry Acta,* 852: 45–54.

Hwang, G., Han ,W. and Park, J. 2008. An electrochemical sensor based on the reduction of screen-printed bismuth oxide for the determination of trace lead and cadmium, *International Journal of electrochemical Science,* 135: 309–316.

Jia, J., Cao, L. and Wang, Z. 2007**.** Nafion/Poly (sodium 4-styrenesulfonate) mixed coating modified bismuth film electrode for the determination of trace metals by anodic stripping voltammetry. *Electroanalysis*, 19: 1845-1849.

Jian, W., Shujun, Y., Yushan, Z., Xiangxue, W., Tao, W., Tongtong, Y., Yuejie, A.,Yuantao C., Tasawar, H., Ahmed, A., and Xiangke, W. 2017. Experimental and theoretical studies of ZnO and MgO for the rapid coagulation of graphene oxide from aqueous solutions. *Journal of Separation and purification Technology*, 184: 88-96.

Jianwei, Z., Fan, M., Lirong, Q., Xiaoya, J. and Caifeng, Y. 2015. Synthesis and characterizati on of MgO/ZnO composite nanosheet for biosensor.*Materials Chemistry and Physics*, 166: 176-181.

Joseph, W. 2008. Electrochemical Sensors for Environmental Monitoring: A Review of Recent Technology, Office of Research and Development of National Exposure Res earch Laborator U.S. *Environmental Protection Agency,* 27(6): 37-102.

Józef, S. and Jan, Ż. 2005. Determination of Lead and Cadmium in Biological Material by Graphite Furnace Atomic Absorption Spectrometry Method. *Bull Vet Inst Pulawy,* 49: 89-92.

Karimi, S., Haghdar, R., Asadiniya, A., Hatefi-Mehrjardi, M.H., Mash hadizadeh,R., Behjat manesh-Ardakani, M., Mazloum-Ardakani, H., Kargar and Zebarjad. 2011. Synthesis and Characterization of Nanoparticles and Nanocomposite of ZnO and MgO by Sonochemical Method and their Application for Zinc Polycarboxylate Dental Cement Preparation. *International Nano Letters*, 1(1): 43-51.

Koudelkova , Z., Tomas, S., Pavlina, A., Zdenek, M., Lubomir, K., David, H. , Lukas , R. and Vojtech, A. 2017. Determination of Zinc, Cadmium, Lead, Copper and Silver Using a Carbon Paste Electrode and a Screen Printed Electrode Modified with Chromium (III) Oxide. *Sensors*, 17: 1832- 1837.

Koudelkova, Z., Zawrotna, N., Pavlina, J., Richtera, L.,and Adam, L. 2016. Using Chromium Modified Carbon Paste Electrode for Heavy Metal Ions Determination. *Mendelnet*, 23: 994-998.

Kundu, T., Mukherjee, M., Chakravorty, D. and Sinha, T. 1998. Growth of nano-α-Fe_2O_3 in a titania matrix by the sol–gel route. *Journal of materials science*, 33(7): 1759-63.

Lahiff, E., Lynam, C. and Gilmartin, N. 2010. The increasing importance of carbon nano tubes and nanostructured conducting polymers in biosensors. *Bioanalytical Chemi stry*, 398: 1575–1589.

Lawal, A. O., Muhammed and D.Damisa, 2006. Assessment of levels of Cu, Cd and Pb in secretion of mammary gland of cow grazed on open fields. *Science World Journal*, 1: 1-8.

Lee, G., Lee, H. and Rhee, C. 2007. Bismuth nano-powder electrode for trace analysis of heavy metals using anodic stripping voltammetry. *Electrochem Commun*, 9: 2514–2518.

Lenntech. 2004. Water Treatment, Published by Lenntech, Rotterdam sewage, Netherlands. Water Purification, 9: 43-47.

Lin, Cui., Jie,W. and Huangxian, J.2015. Electrochemical sensing of heavy metal ions with inorganic, organic and bio-materials. *Biosensors and Bioelectronics*, 63: 276–286.

LI-Quang, Φ., Xino–Ping, W., Wei, L., Xing, T., and Wei-jun, T.,, 2009. The minerals and heavy metals in cow's milk from China and Japan: *Journal of Health Science*, 555(2): 300- 330.

Liu and Zeng. 2003. Hydrothermal synthesis of ZnO nanorods in the diameter regime of 50 nm. *Journal of American Chemical Society*, 125: 4430-4431.

Mahmoud, R., Akram, V. and Zahra, S. 2016. Electroanalytical sensing of Cd^{2+} based on metal–organic framework modified carbon paste electrode. *Sensors and Actuators B* 233: 419–425.

Marcos, R.F.C., Maria, A.C.M., Denise, L. and Renato, C.M. 2014. Optimization and determination of dissolved trace metals (Cu, Cd,Zn and Pb) in rainwater by potentiometric stripping at a southeaster site of Brazil. *Sustainable Environmental Research*, 24(1): 13-21

Mc Bride, M.B. 2003. Toxic metals in sewage sludge-amended soils: has promotion of Mesoporous MgOnanosheets: 1,6-hexanediamin assistedsynthesisand their selectively adsorptive porous magnesium oxide nanoflowers. *Analytical chemistry*, 137: 2183.

Megersa, F. 2014. Natural Dye Sensitized Solar Cells Based on SnO_2/ZnO/Fe_2O_3 Nanocomposite. MSc. Thesis of Haramaya University, Haramaya, Ethiopia

Meseret, A., N. , Megersa, A. M., Tadesse, and Bedessa. 2013. Determination of the levels of selected metals in seeds, flowers, and fruits of medicinal plants used for tapeworm treatment in Ethiopia. *Toxicological and Environmental Chemistry*, 95:82–100. doi:10.1080/02772248.2012.744022.

Mikkelsen, O. and Schroder, K.H. 2004. Voltammetric monitoring of bivalent iron in waters and effluents, using a dental amalgam sensor electrode. *Electroanalysis*, 16: 386-390.

Nazari M and Halladj R. 2014. Adsorptive removal of fluoride ions from aqueous solution by using sonochemically synthesized nanomagnesia/alumina adsorbents:An experimental and modeling study. *Journal of the Taiwan Institute of Chemical Engineers*, 45(5): 2518-25.

Ogabiela, E. E., Yebpella, G. G., Ade-Ajayi, A. F., Mmereole, U. J., Ezeayanaso, C., Okonkwo, E. M., Ahola, D. O., Udiba, U. U., Mahmood, A. and Gandu, I. 2010. Determination of the level of some elements in edible oils sold in Zaria, Northern Nigeria. *Global Journal of Pure and Applied Sciences*, 6 (3): 325-331.

Pedro, H.C.C., Kestur, G. S. and Fernando W. 2009. Nanocomposites: Synthesis, Structure, Properties and New Application Opportunities. *Materials Research*, 12 (1):1-39.

Ping .J. F., Wu. J. and Ying Y. B. 2012. Determination of trace heavy metals in milk using an ionic liquid and bismuth oxide nanoparticles modified carbon paste electrode. *China Science Bull*, 2012, 57: 1781-1787, doi: 10.1007/s11434-012-5115-1.

Ping. J. F., Wu, J. and Ying. Y. B. 2011. Evaluation of trace heavy metal levels in soil samples using an ionic liquid modified carbon paste electrode. *Journal of Agricultral and Food Chemistry*, 59: 4418–4423.

Risher, J. and DeWoskin, R. 1999. Toxicological profile for mercury. *Agency for Toxic Substances & Disease Registry.*

Sahoo, P., Panigrahy,B., Sahoo,S., Satpati,A., Li,D. and Bahadur,D. 2013. Electrochemical sensing of heavy metal ions with inorganic,organic and bio-materials. *Biosens and Bioelectronics*, 43: 293–296.

Sailus, M. and Mugendi, M.I. 2014. Determination of the levels of selected heavy metals in soil and in khat (cathaedulisforsk) grown in Kenya. *Journal of Environmental, Agricultural and Food Chemistry*, 17: 87-95.

Samara, S. and H. Richard, 2009. Heavy metal toxicity, medicine Specialist greater than Emergency Medicine Toxicology. New York.

Sarunya, K., Pongsaton, A. k. and Sumetha, S. 2015. Structural, optical and photo catalytic pr operties of MgO/ZnO nanocomposites prepared by a hydrothermal method. *Materials Sciencein Semiconductor Processing*, 39: 515–520.

Sathyamoorthy, T., Sivaruban and Barathy. 2016. Assessment of Heavy Metal Pollution and Contaminants in the Cattle Meat. *Journal of Industrial Pollution Control*, 32(1): 350-355.

Semaghuil, B., Simona, D., Stanciu, G. and Soceanu, A. 2008. Determination of Major and Minor Elements in milk through ICP-AES. *Environmental Engineering and Management Journal*, 6: 805-808.

Silveira, T.A.DA. Araujo, D.F.d. Marchini, C. Moreti, A.C.C.C. and olinda, R.A. 2013. Detection of Metals by Differential Pulse Anodic Stripping Voltammetry (DPASV) in Pollen Collected From a Fragment of the Atlantic Forest in Piracicaba/SP. *Ecotoxic ology Environmental Contamintion,* 8(2): 31-36. doi: 10.5132/eec.2013.02.005.

Soheila,S., Mahmoud, E. and Safar, A. B. 2016. Modified carbon paste electrode with ionic liquid and SiO_2 nanoparticles for potentiometric determination of Copper (II) ions in real samples. *International Journal of Medical Research & Health Sciences,* 5(8): 326-331.

SowriBabu, A., Ramachandra, R. and Venugopal, R. 2015.GreenemissionfromZnO/MgO nanocomposite due to Mg diffusion at the interface. *Journal of Luminescence*, 158: 306–312.

Stankic, S., Suman, S., Haque, .F and Vidic, J. 2016. Pure and multi metal oxide nanopartic les: synthesis, antibacterial and cytotoxic properties. *Journal of Nanobiotechnology*, 14(1):73.

Stozhko, N.Y., Malakhova, N.A., Fyodorov, M.V. and Brainina, K.Z. 2008. Modified carbon containing electrodes in stripping voltammetry of metals. *Journal of Solid State Electrochemistry,* 12: 1185-1204.

Subhash, B., Kondawar, Smita, A., Acharya and Sanjay, R. D. 2011. Microwave assisted hydrothermally synthesized nanostructure zinc oxide reinforced polyanniline nanocom posite. *Advanced Materials Letters*, 2(5): 362-367.

Švancara, I.,Vytřas ,K. and Kalcher, K. 2009. Carbon paste electrodes in facts, numbers, and notes: A review on the occasion of the 50-years jubilee of carbon paste in electrochemistry and electroanalysis, 21: 7–28 20.

Švancara, Monica, F., Matěj, S., Lucie, B., Eva, S., and Mihaela, B. 2010. Carbon Paste Elec trodes Modified with a Reaction Product Obtained by Hydrolysis of an Antimony(III) Salt. *Sensing in Electroanalysis*, 5: 09-125.

Sylwia, S. and Witold, C. 2015. Application of a Graphene Oxide–Carbon Paste Electrode for the Determination of Lead in Rainbow Trout from Central Europe. *Food Analysis Methods*, 8:635–642.

Tanuja, S.B., Kumara S. and Vasantakumar, P. K. 2017. Electrochemical determination of paracetamol in presence of folic acid at nevirapine modified carbon paste electrode: A cyclic voltammetric study. *Journal of Electro analytical Chemistry,* 798: 17–23.

Tercier, W.L., Confalonieri, F., Riccardi, G., Sina, A., Noel, S., Buffle, J. and Graziottin, F. 2005. Multi physical and chemical profiler for real time in situ monitoring of trace metal speciation and master variables: Development, validation and field applications. *Marine Chemistry*, 97: 216-235.

Tesfaye, T.W., Sibusiso, Q., Priscilla, G.B. and Emmanuel I. I. 2016. Electrode Material Properties and Modelling of 1- Methyl-3-octylimmidazolium

Tilahun, B., Zemene, A. and Alle, M. 2015. Determinations of the level of essential and non-essential metals in rice and soil samples**.** *International Journal of Modern Chemistry and Applied Science***,** 2(1): 65-72.

Tokusoğlu, Ö., Aycan ,S. and Akalin, S. 2004. Simultaneous differential pulse polarographic determination of cadmium, lead, and copper in milk and dairy products. *Journal of Agriculture and Food Chemistry*, 52: 1795–1799.

Tsoumbaris, P. and H. Tsoukali-Papadopoulou, 1994. Heavy Metals in common foodstuff: Qualitative analysis. *Bulletin of Environmental Contamination and Toxicology*, 53: 267-269.

Vennila, S., Jesurani, Sr. S., Priyadharshini, M. and Ranjan, M. 2016. Eco-Friendly Synthesis Of Metal Oxide Nanoparticles Using Carissa Carandasfruitextract, *World Journal of Pharmaceutical Research*, 5 (7): 806-812.

Viswanatha, R., Venkatesh, T.G., Vidyasagar, C.C.and Arthoba Nayaka, Y. 2012. Preparati on and Characterization of ZnO an Mg-ZnO nanoparticle. *Archives of Applied Science Research*, 4 (1):480-486.

Volesky, B. and H. May-Phillips, 1995. Biosorption of heavy metals by Saccharomyces Cerevisiae. *Journal of applied Microbiology Biotechnology*, 42:797-806.

Wang, H., Yu, Z., Wang, Z., Hao, H., Chen, Y. and Wan, P. 2011. Preparation of a preplated bismuth film on Pt electrode and its application for determination of trace aluminum(iii) by adsorptive stripping voltammetry. *Electroanalysis*, 23: 1095–1099.

Wang, J. 2005. Stripping Analysis at Bismuth Electrodes: A Review. *Electroanalysis*, 17: 1341-1346.

Warner, M.G., Fryxell, G.E., Addleman, R.S., and Timchalk, C. 2008. Removal of Cadmium Ion froWastewater by Nano-metal Oxides: *A Review. Journal of electrochemistry*, 133: 348–355.

Wei, B. G. and Yang, L. S. 2010. A review of heavy metal contaminations in urban soils, urban road dusts and agricultural soils from China. *Journal Micro chemical*, 94: 99–107.

Wenshu, Z., Caihong, L., Chong, S. and Xiaodi, Y. 2016. Simultaneously determination of trace Cd^{2+} and Pb^{2+} based on L-cysteine/graphene modified glassy carbon electrode. *Food Chemistry*, 192: 351–357.

Win, M.H. 2007. Infrared Spectroscopy of Zinc Oxide and Magnesium Nanostructures used drug in water using ZnO nanoparticles; Degree of Doctor of Philosophy Washington State University Materials Science Program. *Journal of luminium*, 130:2327–2331.

World Health Organization/WHO, 1996. Trace elements in human nutrition and health, (A report of a re-evaluation of the role of trace elements in human health and nutriation). Geneva.

Yahaya, M.I., Ezor, G. C., Musa Y. F. and Muhamad, S. Y. 2010. Analysis of heavy metals concentration in road side soils in Yauri, Nigeria. *African journal of pure and applied chemistry*, 4: 3.

Yan, W., Ran, Y., Xin-Yao, Y., Lun, W., Jin-Huai, L. and Xing-Jiu, H. 2012. Stripping voltammetry study of ultra-trace toxic metal ions on highly beneficial use discounted the risks. *Advances in Environmental Research*, 8: 5–19.

Yang, H., Shi. R., Zhang, K., Hu, Y., Tang, A. and Li, X. 2005. Synthesis of WO_3/TiO_2 nanocomposites via sol–gel method. Journal of Alloys and Compounds, 398(1):200-2.

Yantasee, W., Hongsirikarn, K., Warner, C.L., Choi,D., Sangvanich,T., Toloczko,M.B. ,Zhengcui, W., Chengrong,X., Huamao, C., Yaqin, W., Hao, Y., Yin,Y. and Feng, G. 2013. Applications on electrochemical detection of toxic metal ions. *Journal of Physicsand Chemistry of Solid*, 74:1032–1038.

Yoseph Bereket.2009. Electrochemical Detection of Methyl Parathion using poly-(4-amino-3-hydroxynaphthalene-1-sulphonicacid) Modified Glassy Carbon Electrode. MScProject, Addis Ababa University, Addis Ababa, Ethiopia.

Zhang, H., and Chen, G. 2009. Potent antibacterial activities of Ag/TiO_2 nanocomposite powders synthesized by a one-pot sol- gel method. *Journal of Environmental science & technology*, 43(8): 2905-10.

Zhuo, G., Dong-di, L., Xian-ke, L., Ya-hui, L., Qi-Nai, Z., Meng-meng, L., Yang-ting Z., Tian-shuai, S. and Chi, M. 2017. Simultaneous determination of trace Cd(II), Pb(II) and Cu(II) by differential pulse anodic stripping voltammetry using a reduced grapheme oxide-chitosan/poly-L-lysine nanocomposite modified glassy carbon electr-ode. *Journal of Colloid and Interface Science*, 490: 11–22.

7. APPENDICES

Appendices Table 1. The effect of scan rate on peak current using GCE in 2 mM $K_3Fe(CN)_6$

Scan rate (mV/s)	i_{ap}(µA)	E_{pa} (mV)	i_{pc} (µA)	E_{pc} (mV)	i_{ap}/i_{cp}	ΔE_p (mV)	$(E_{pa}+E_{pc})/2$
10	6.17	253	-9.83	185	0.62767	68	0.219
25	11.02	255	-14.03	178	0.78546	77	0.2165
50	18.99	257	-19.65	179	0.96641	78	0.218
75	19.89	265	-20.93	175	0.95031	90	0.22
100	23.3	269	-24.19	170	0.96320	99	0.2195

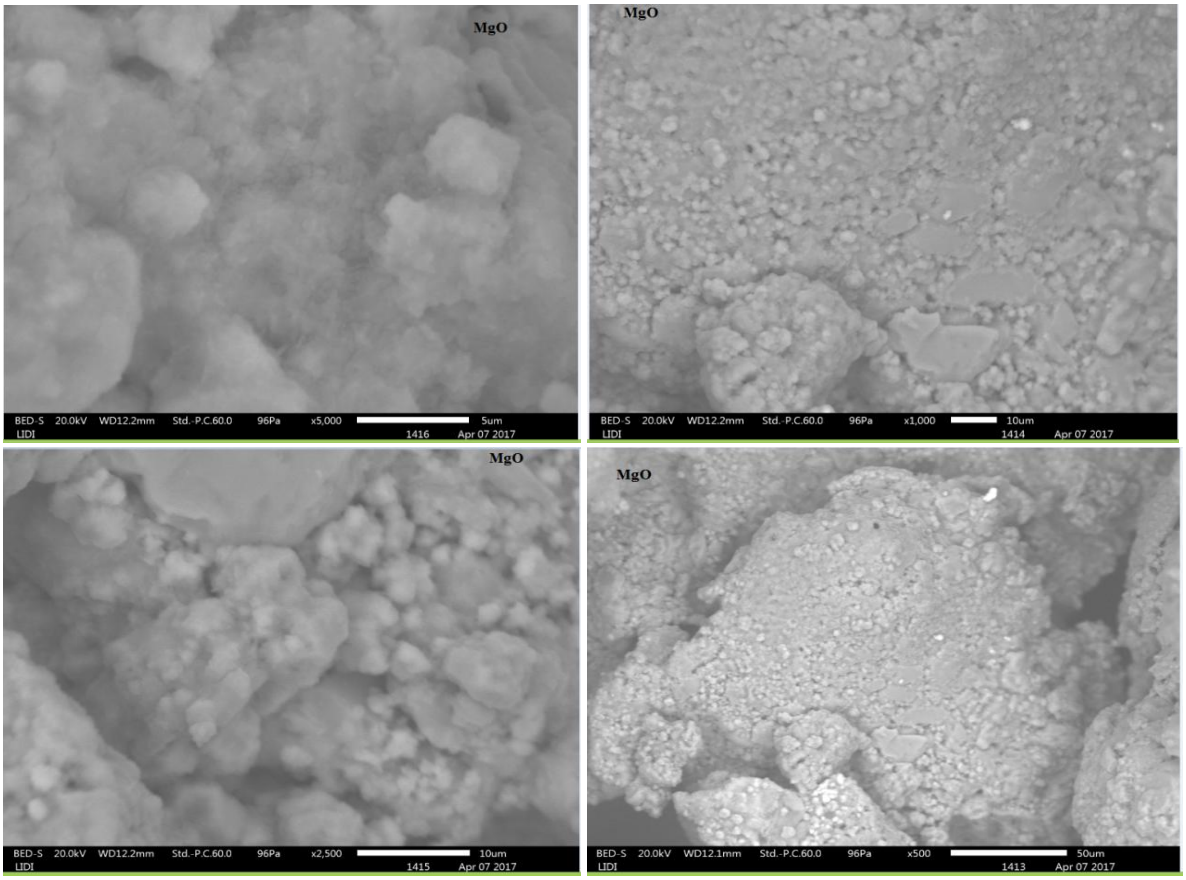

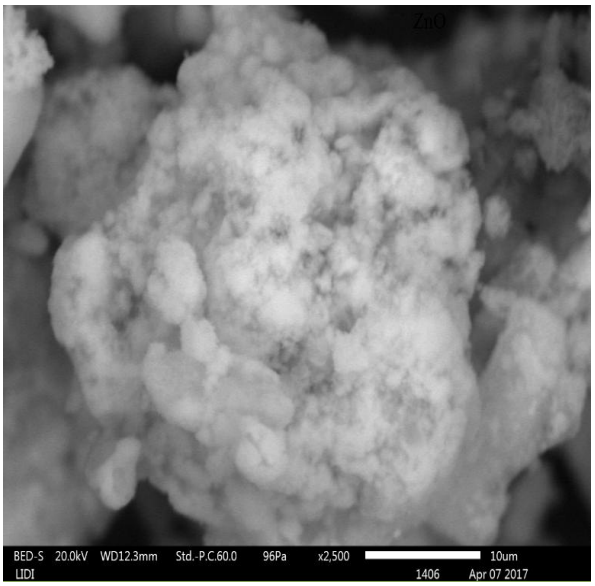
ZnO
BED-S 20.0kV WD12.3mm Std.-P.C.60.0 96Pa x2,500 10um
LIDI 1406 Apr 07 2017

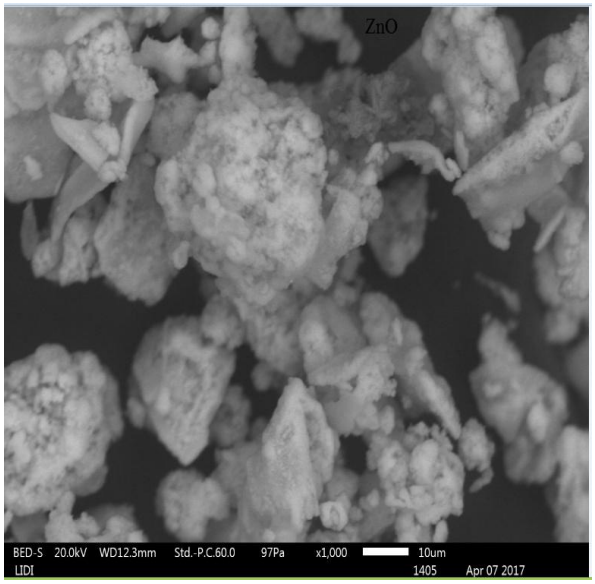
ZnO
BED-S 20.0kV WD12.3mm Std.-P.C.60.0 97Pa x1,000 10um
LIDI 1405 Apr 07 2017

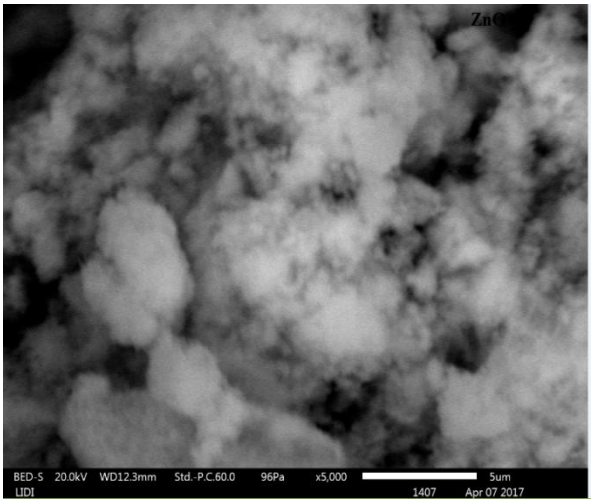
ZnO
BED-S 20.0kV WD12.3mm Std.-P.C.60.0 96Pa x5,000 5um
LIDI 1407 Apr 07 2017

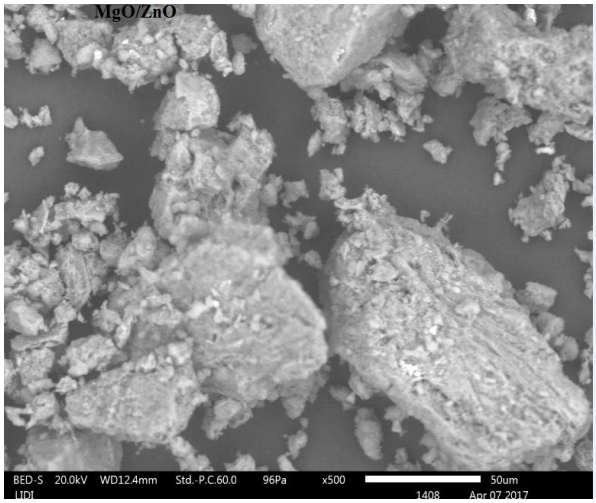
MgO/ZnO
BED-S 20.0kV WD12.4mm Std.-P.C.60.0 96Pa x500 50um
LIDI 1408 Apr 07 2017

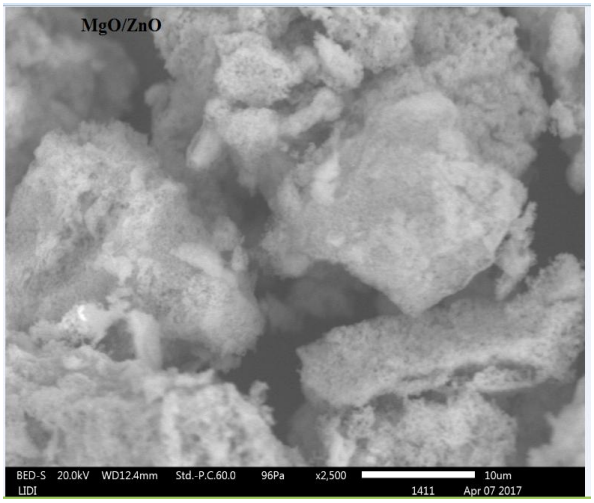
MgO/ZnO
BED-S 20.0kV WD12.4mm Std.-P.C.60.0 96Pa x2,500 10um
LIDI 1411 Apr 07 2017

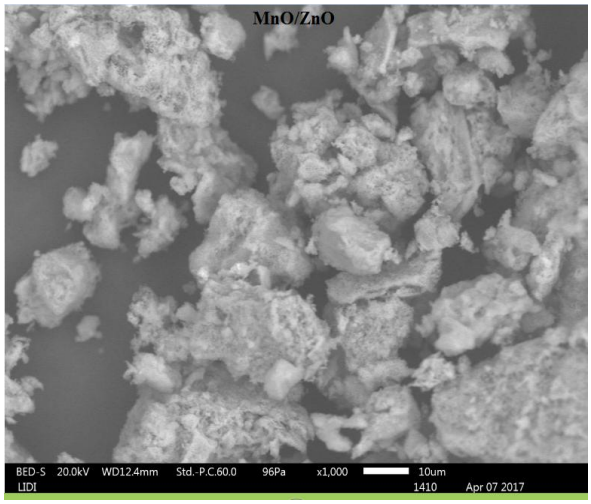
MnO/ZnO
BED-S 20.0kV WD12.4mm Std.-P.C.60.0 96Pa x1,000 10um
LIDI 1410 Apr 07 2017

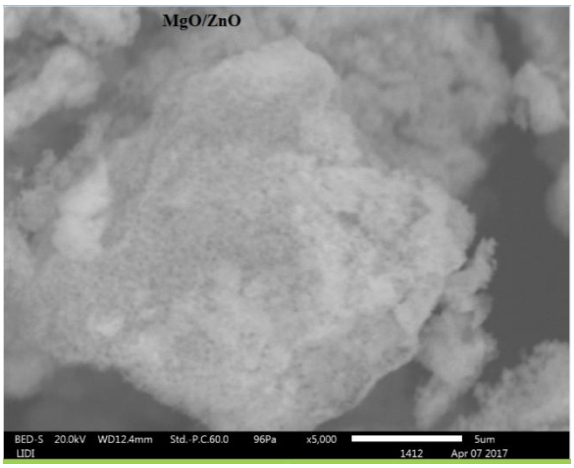

Appendicis figure 1. Different magnification image of SEM of MgO, ZnO and MgO/ZnO NCPs

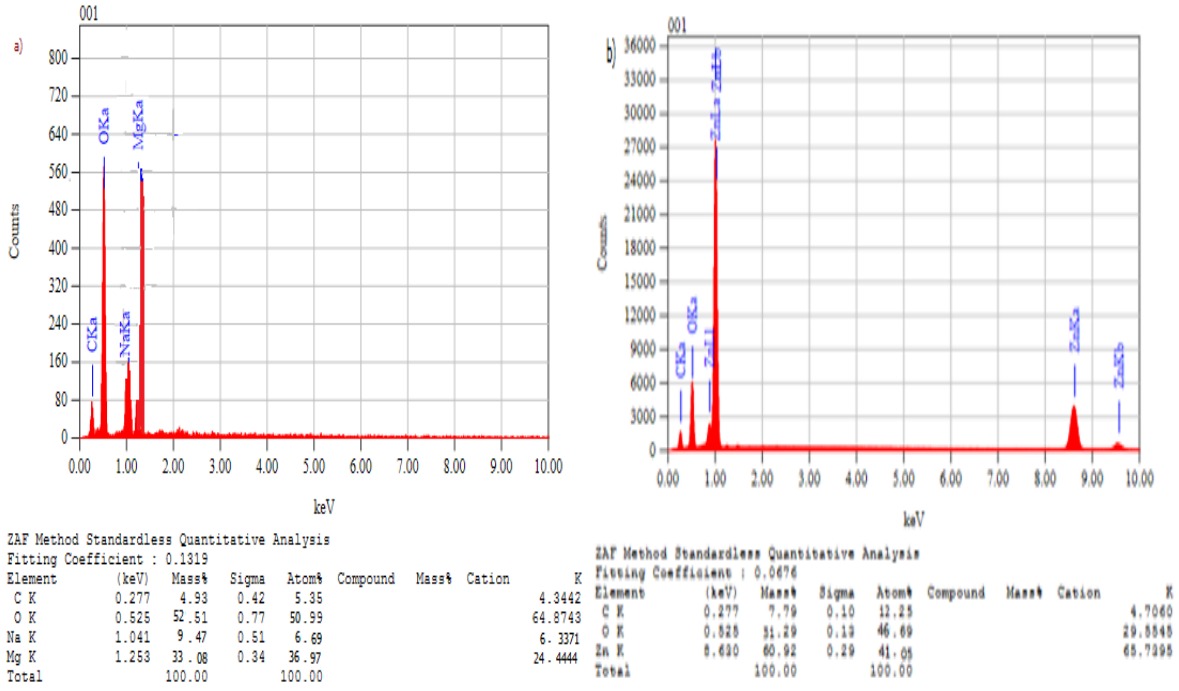

Appendices figure 2. The EDX data of MgO a) and ZnONPs (b).

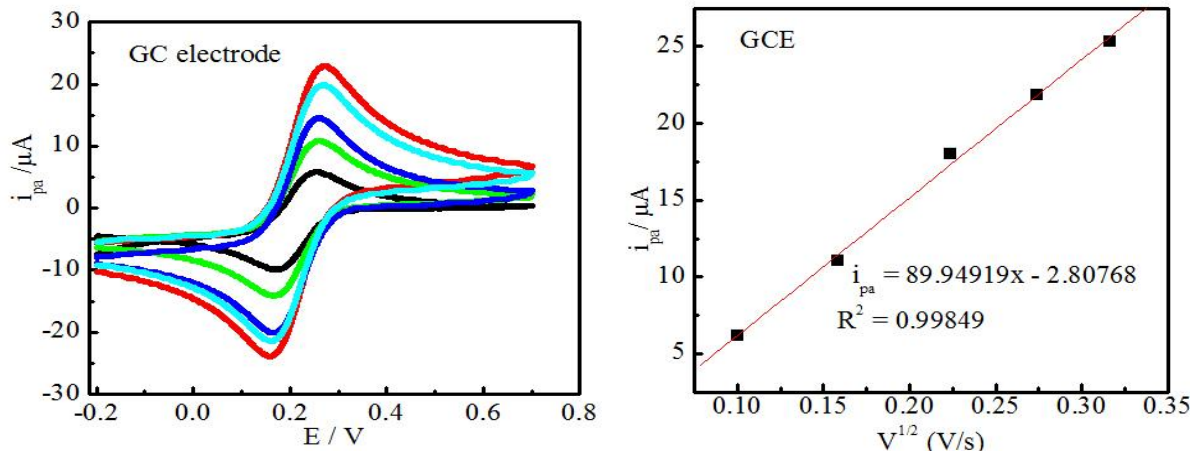

Appendices figure 3 . Cyclic voltammograms of GCE, 2 mM of $K_3Fe(CN)_6$ + 0.1 M KCl at different scan rates 10, 25, 50, 75 and 100 mVs^{-1} and plot of peak current vs square root of scan rate for CPE.

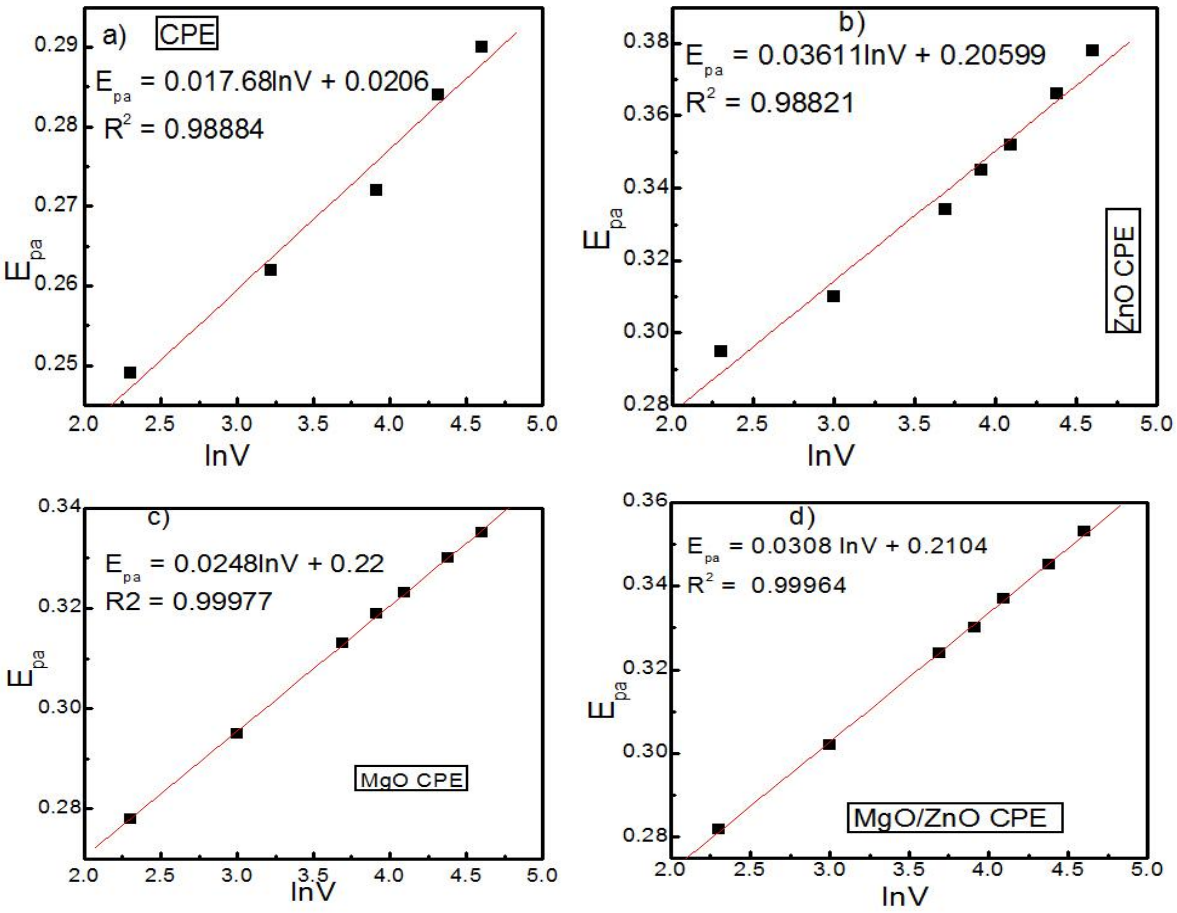

Appendicis figure 4. E_{pa} vs lnv graph of CPE, ZnOCPE , MgOCPE & MgO/ZnO/CPE

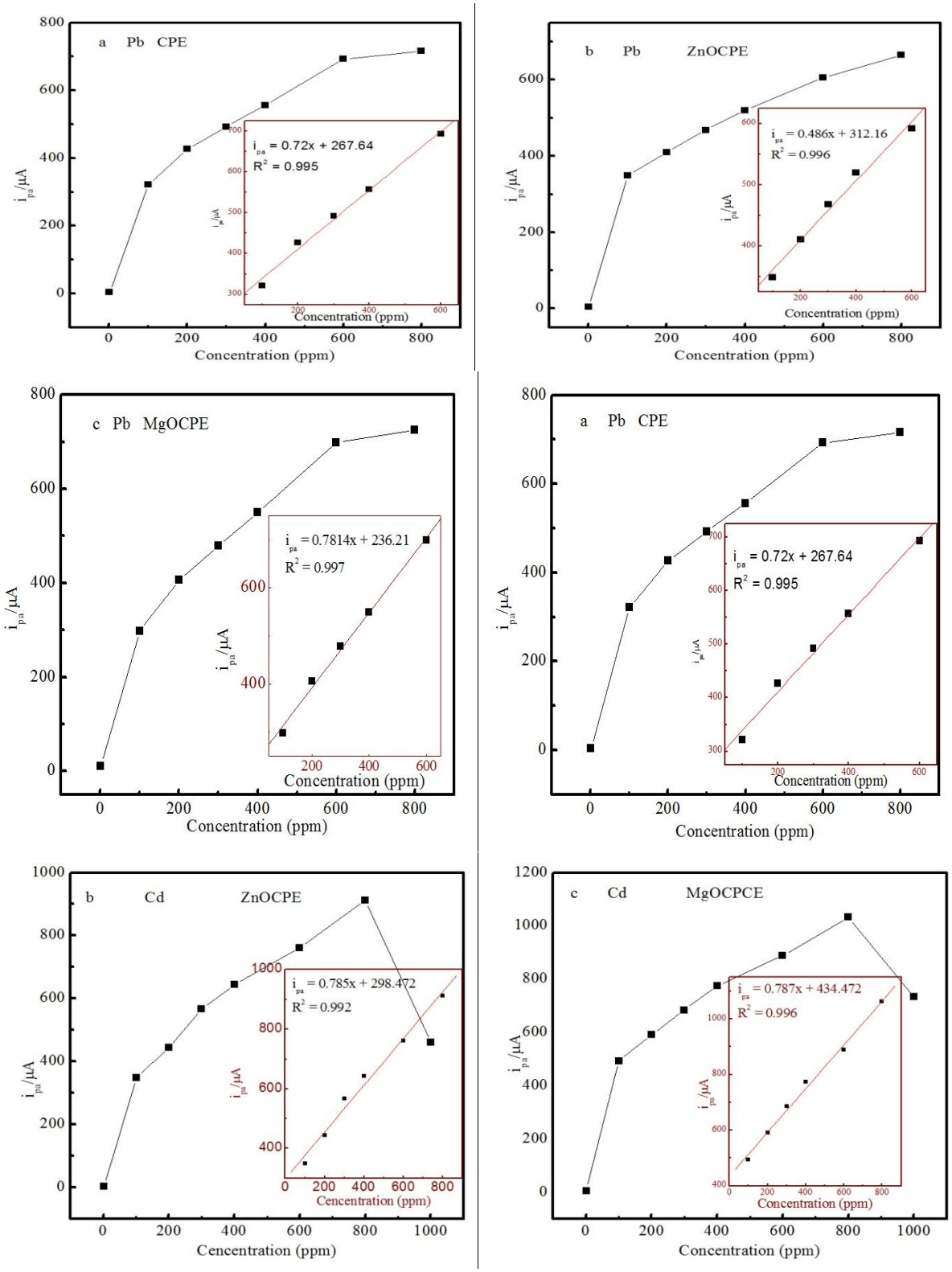

Appendicis figure 5. Plot of peak current *versus* concentration for Cd and Pb on different MCPE obtained from ASV at 0.1M acetate buffer pH 4.5, deposition time 90 Sec and scan rate of 50mV/s